Enhanced Activities of Metal Oxide Electrocatalysts for Clean Energy Generation and Storage

Robin Forslund

The University of Texas at Austin

Second International Conference of Young Scientists

Moscow Region, Russia

September 18th, 2017

Skoltech

Skolkovo Institute of Science and Technology

LOMONOSOV MOSCOW STATE UNIVERSITY 1755 MSU

THE UNIVERSITY OF TEXAS AT AUSTIN

Oxygen Electrochemistry

Oxygen Chemistry is Ubiquitous

- Electrolyzers for H_2 generation
- Metal-air batteries (Zn-air, Li-air)

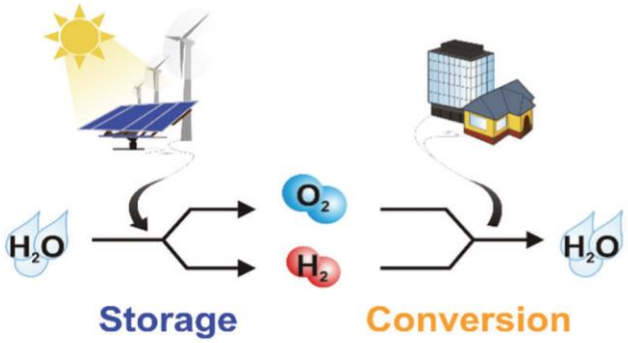

oxygen evolution reaction (**OER**)

$4OH^- \rightarrow O_2 + 2H_2O + 4e^-$

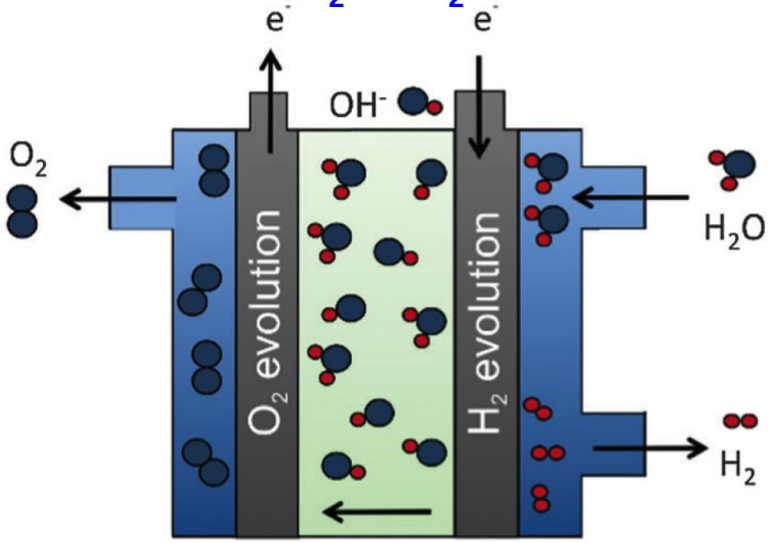

Electrolyzer

oxygen reduction reaction (**ORR**)

$O_2 + 2H_2O + 4e^- \rightarrow 4OH^-$

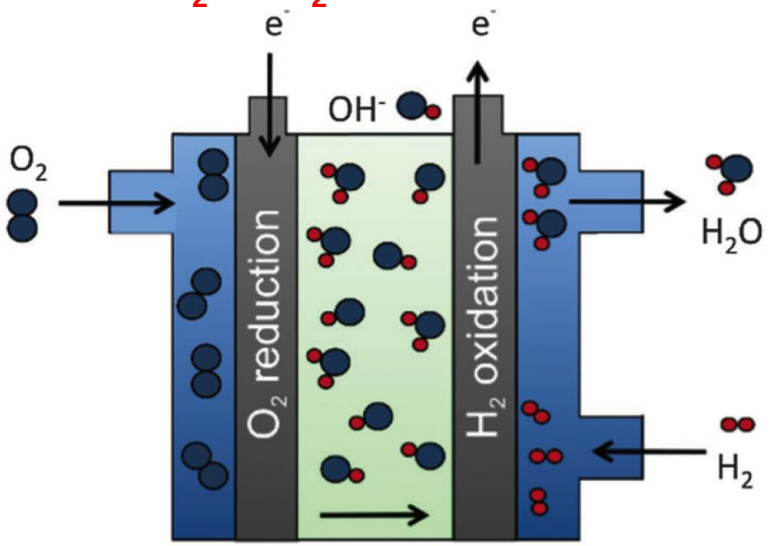

Fuel Cell

Hong, W. T.; Grimaud, A.; Suntivich, J.; Shao-Horn, Y. *Energy Environ. Sci.*, **2015**

OER & ORR Thermodynamics

- "kinetically sluggish" reactions require large overpotentials ($\eta \geq 300$ mV)
- Large overpotentials result in lower power, device efficiency

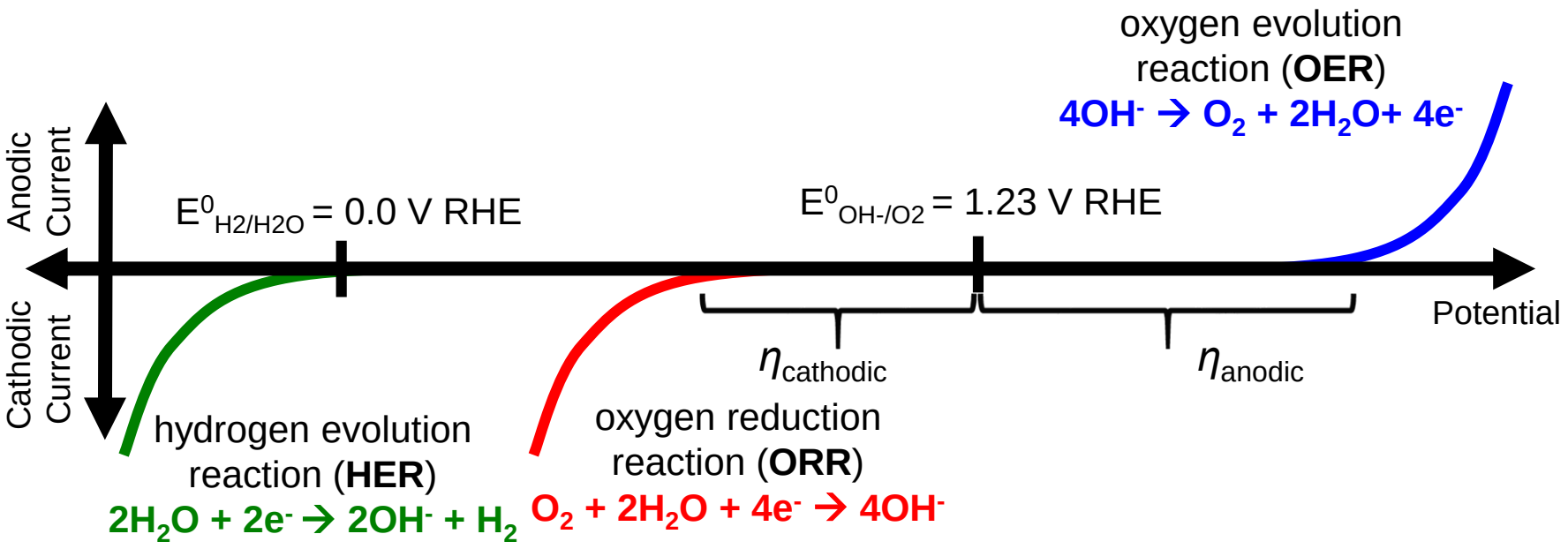

Catalyst materials

- Materials capable of both OER and ORR for regenerative fuel cells → '**bifunctional**' catalysts
- Alkaline electrolyte enables **non-precious metal oxides** → **Perovskites**

What is a Perovskite?

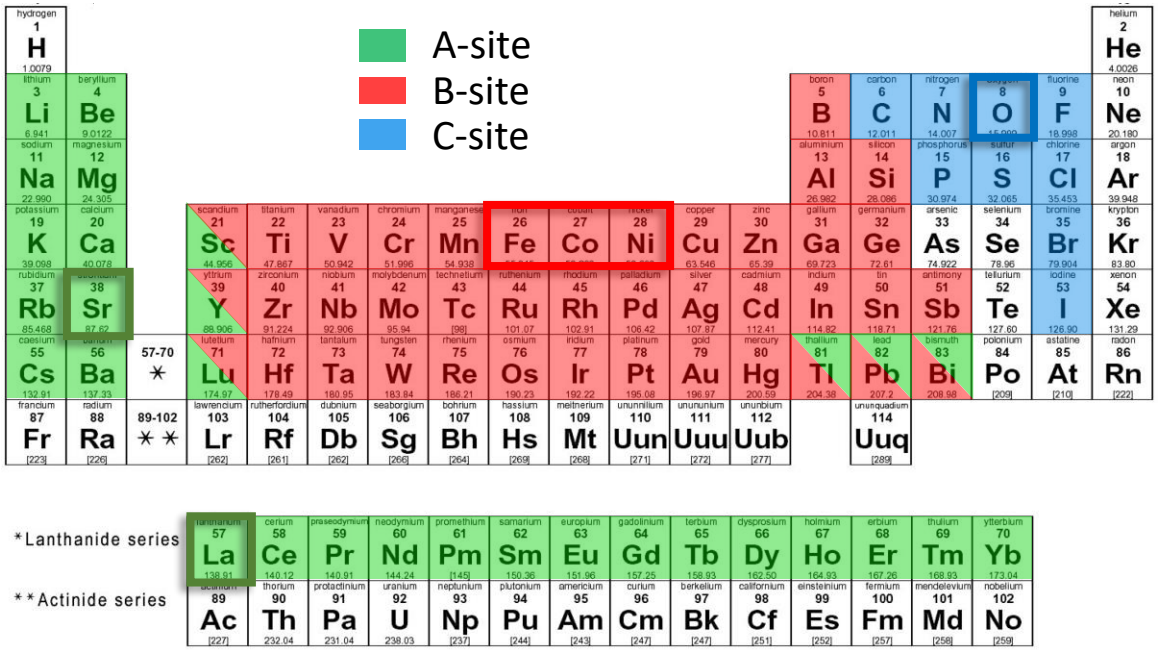

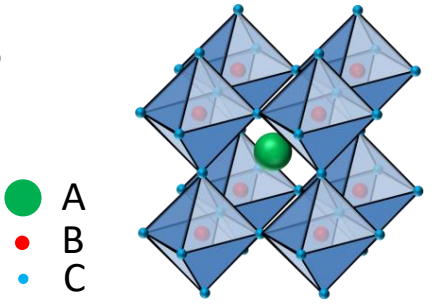

Perovskite: ABC_3

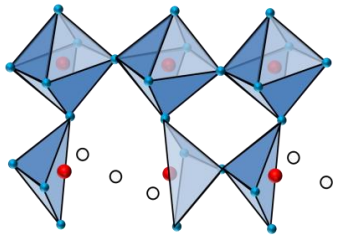

Brownmillerite: $A_2B_2C_5$

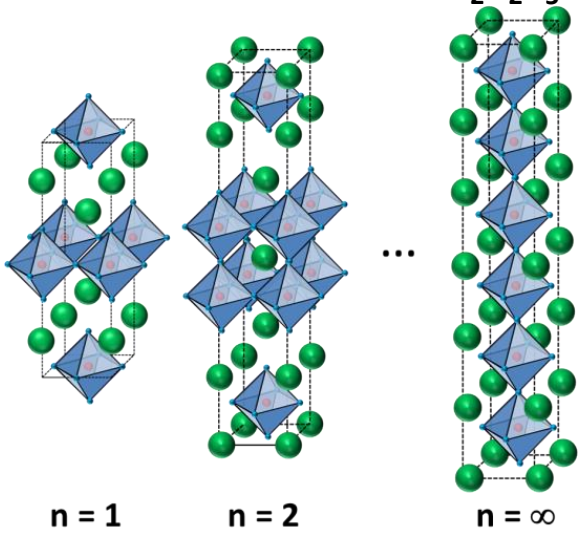

Ruddlesden-Popper: $(AC)(ABC_{3\pm\delta})_n$

- Simple Cubic with formula ABC_3
- Generally **form at high temperatures** (>700° C), low S.A.
- Mixed ionic-electronic conductors
- Only B-Site is catalytically active

Background & Structure

Perovskite-type oxide ABO_3

- B-site atom (1st row transition metal) in 6-fold octahedral coordination
- BO_6 units breaks *d* manifold degeneracy
- Cubic, hexagonal -> rhombohedral crystal structure, influenced by:
  - ionic sizes
  - B 3*d* – O 2*p* interactions
  - J-T distortions

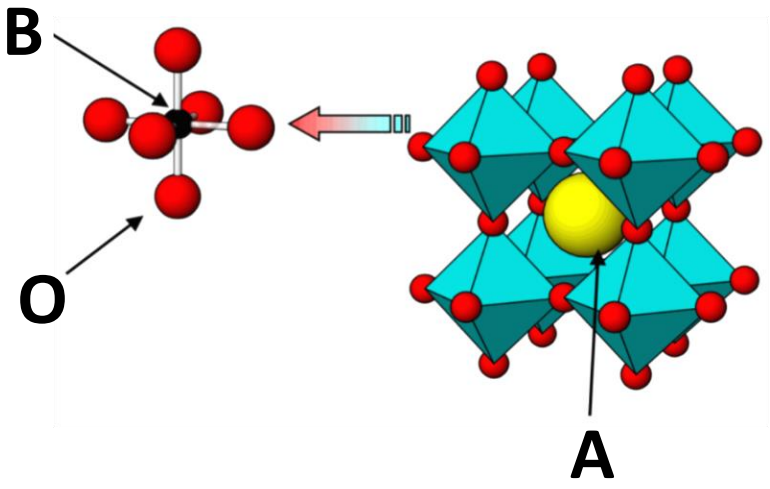

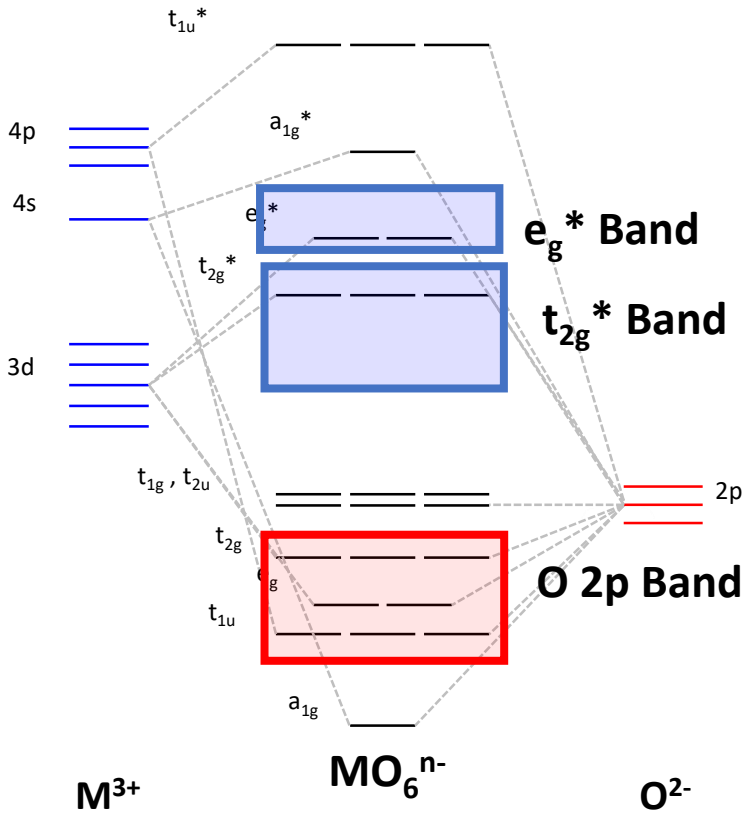

Synthesis

Goal:

- Purity: overcome dissimilar rates of hydrolysis for A and B site cations (ABO_3)
- Surface-Area: stabilize nanoparticles precursors through electrostatic and steric interactions

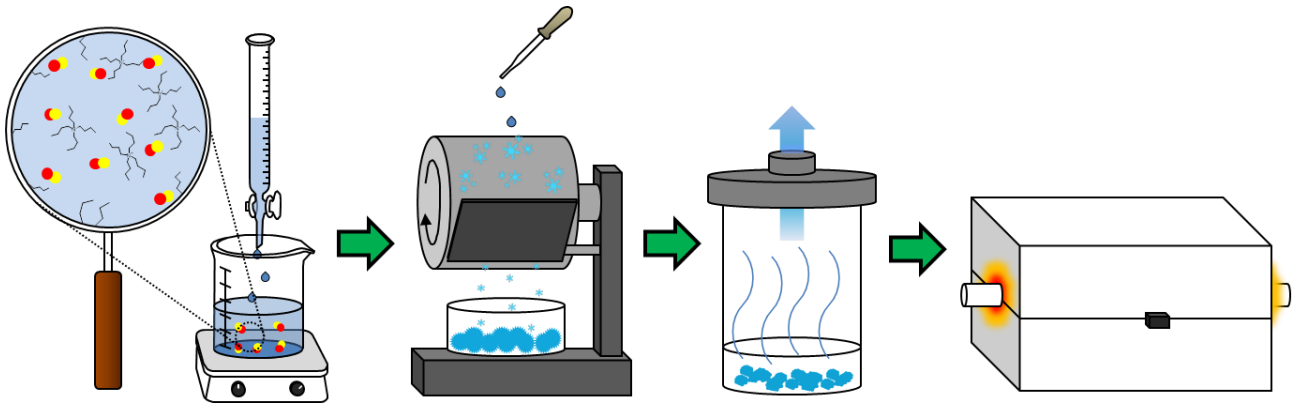

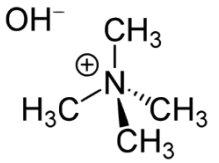

(TMAOH)

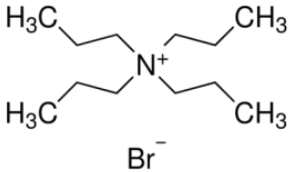

(TPAB)

Strategy:

- Rapid hydrolysis in presence of excess [OH^-]
- Thin-film freezing rates > aggregation time of nanoparticle precursors
- Lyophilization to avoid capillary condensation / maximize inter-particle distance
- Crystallization in tube furnace

Electrode Testing

- Ball mill to break up particles
- Support perovskite on carbon (30 wt%) by ball-milling
- Suspend catalyst in EtOH with Na-substituted Nafion binder and sonicate
- Dropcast 51 μg/cm^2 of composite onto 5 mm GCE and let dry overnight

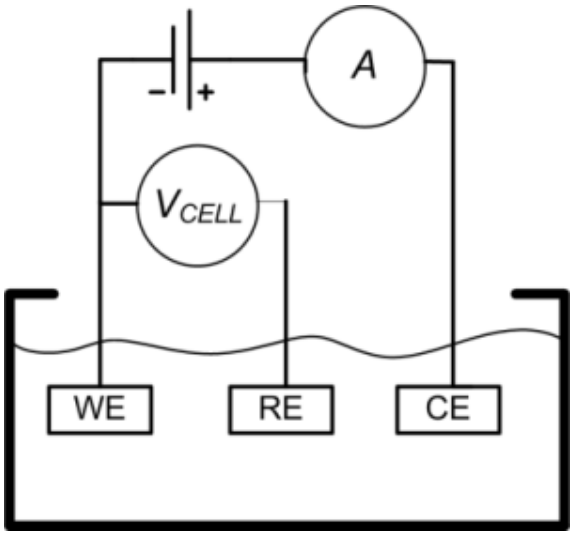

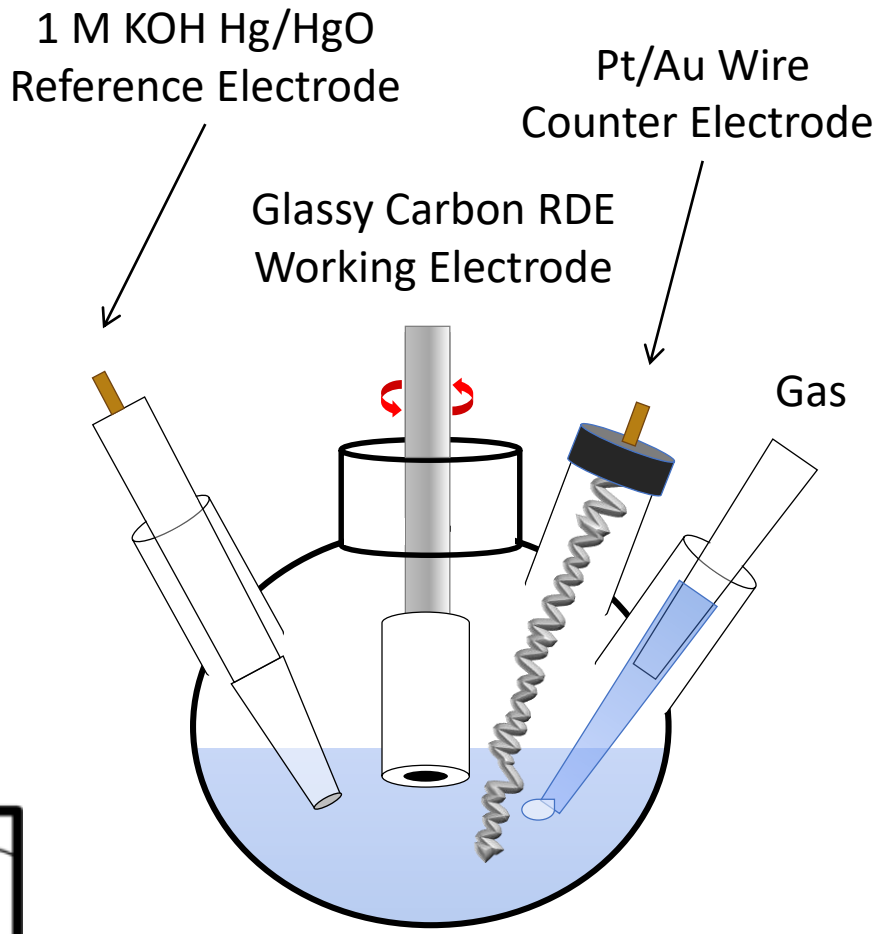

RHE potential measurement

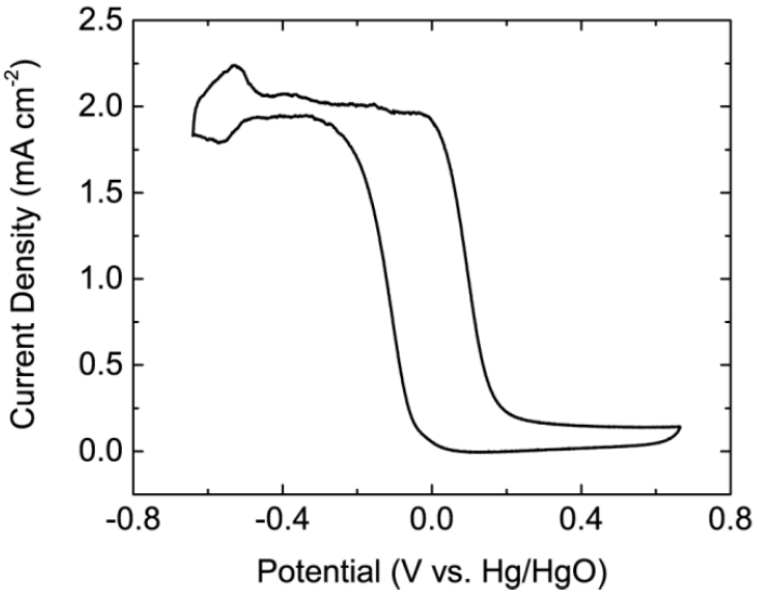

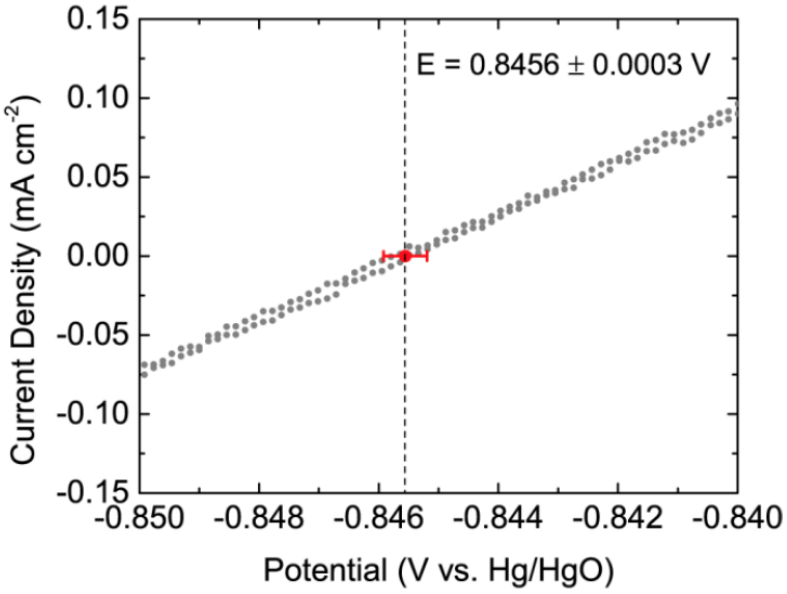

- Use a Pt RDE as the working electrode
- Clean Pt RDE by cycling in Ar-saturated 0.1 M KOH until a stable CV is observed
- Saturate the solution with H_2 and cycle through H_2 evolution/reduction
- Then our potential vs. RHE is:
  - $E_{RHE} = E_{Hg/HgO} + (0.8456\ V)$
- Use positive resistance feedback method to measure solution resistance: 46 ohms in 0.1 M KOH

Early Work

- N-doped carbon (NC) consistently best support
- $LaCoO_3$/NC more bifunctional than Ru or Pt
- Nanostructuring perovskites with phase purity increases both the specific (mA cm^{-2}_{ox}) and mass (mA g^{-1}_{ox}) activities

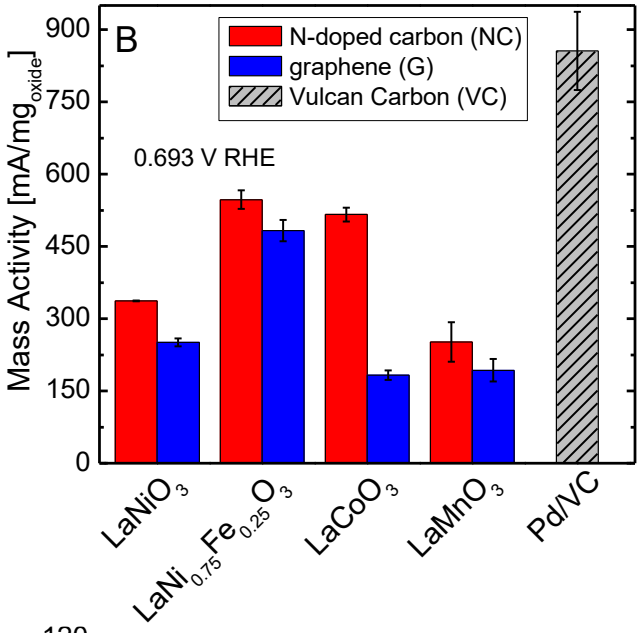

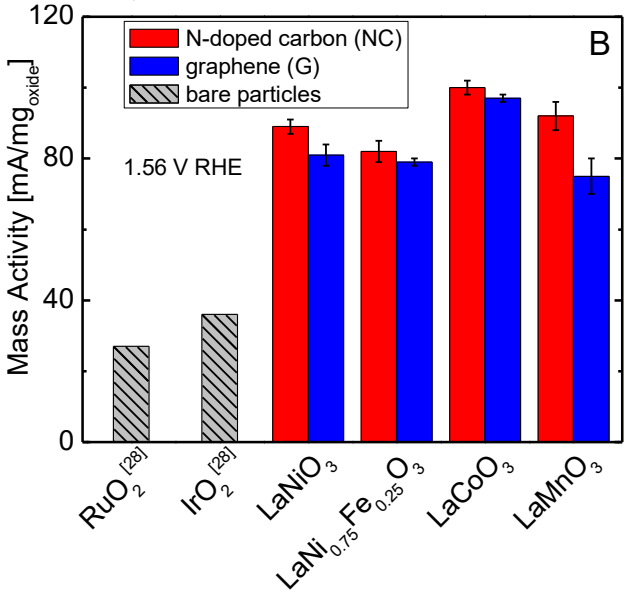

Material	ORR Potential (V) vs RHE @ j = -3 mA/cm²	OER Potential (V) vs RHE @ j = 10 mA/cm²	ΔE (V) Bifunctionality
$LaNiO_3$/NC	**0.64**	**1.66**	**1.02**
$LaNi_{0.75}Fe_{0.25}O_3$/NC	**0.67**	**1.68**	**1.01**
$LaCoO_3$/NC	**0.64**	**1.64**	**1.00**
20% Ir/C¥	**0.69**	**1.61**	**0.92**
20% Ru/C¥	**0.73**	**1.62**	**1.01**
20% Pt/C¥	**0.86**	**2.02**	**1.16**

Hardin, Mefford, KPJ, KJS et al., J. Phys. Chem. Letters (13), Chem. Mater. **(14)**

Catalyst Design Principles

e_g filling of 1 proposed as governing descriptor of OER/ORR activity – Sabatier principle

- Filling >1 → more antibonding → OH^- too weakly bound
- Filling <1 → more bonding → OH^- too strongly bound

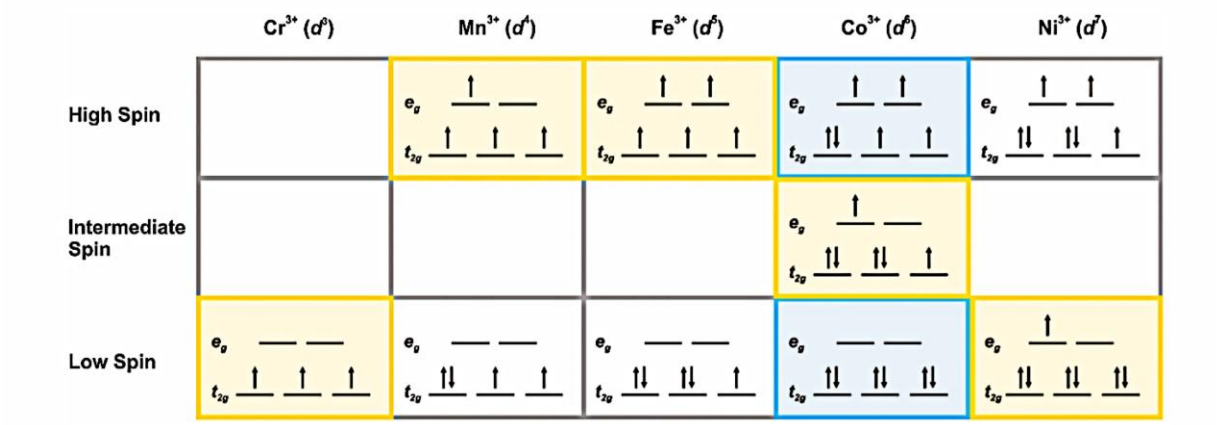

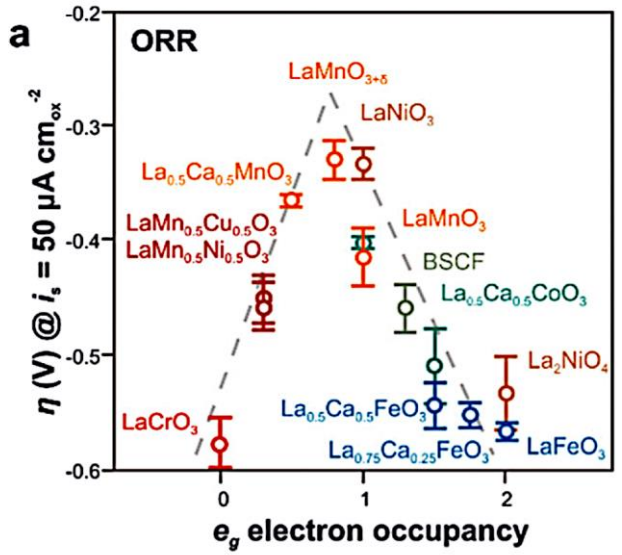

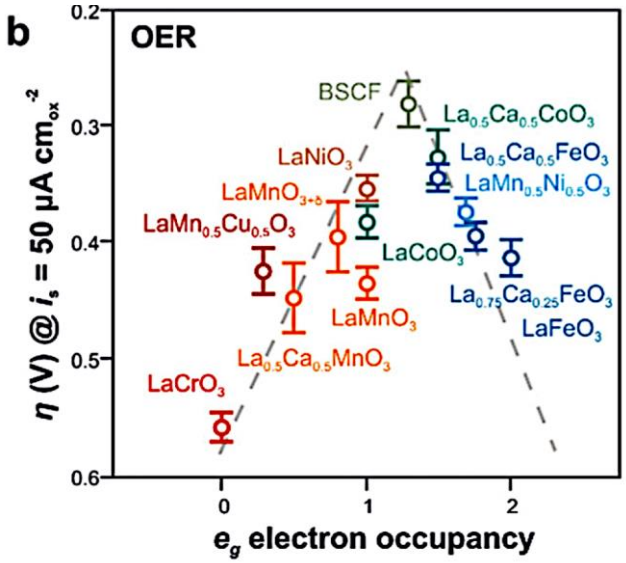

Hong, W. T.; Grimaud, A.; Suntivich, J.; Shao-Horn, Y. *Energy Environ. Sci.*, **2015**

- XPS shows lattice oxide ions in protonated state (OH^- signature in O 1s)
- ^{18}O studies on Li-NiO, RuO_2, IrO_2 indicate that evolved O_2 from lattice
- Proposed RDS for OER is peroxide (HOO^-) formation: involving O_{ads} and OH^-
- Lattice Hydroxides contribute OH^- to peroxide formation → more energetically favorable than solution OH^-

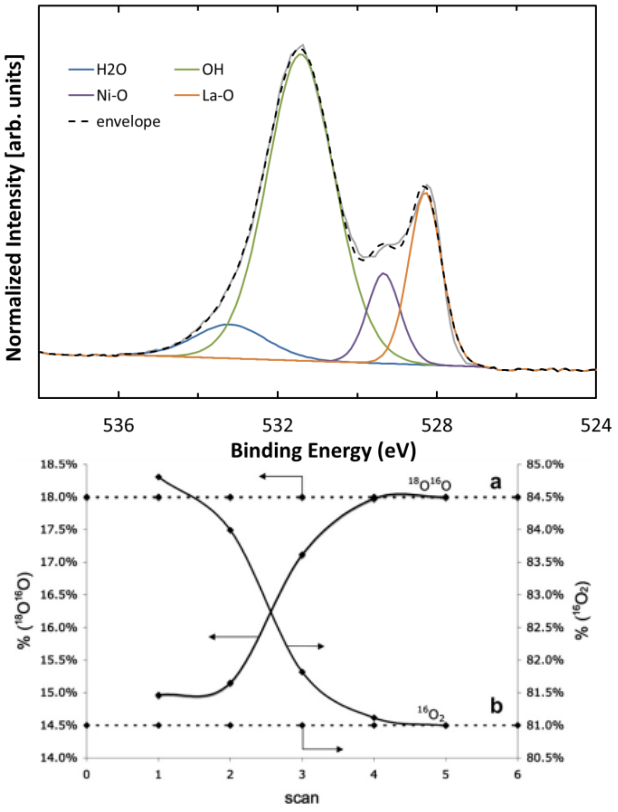

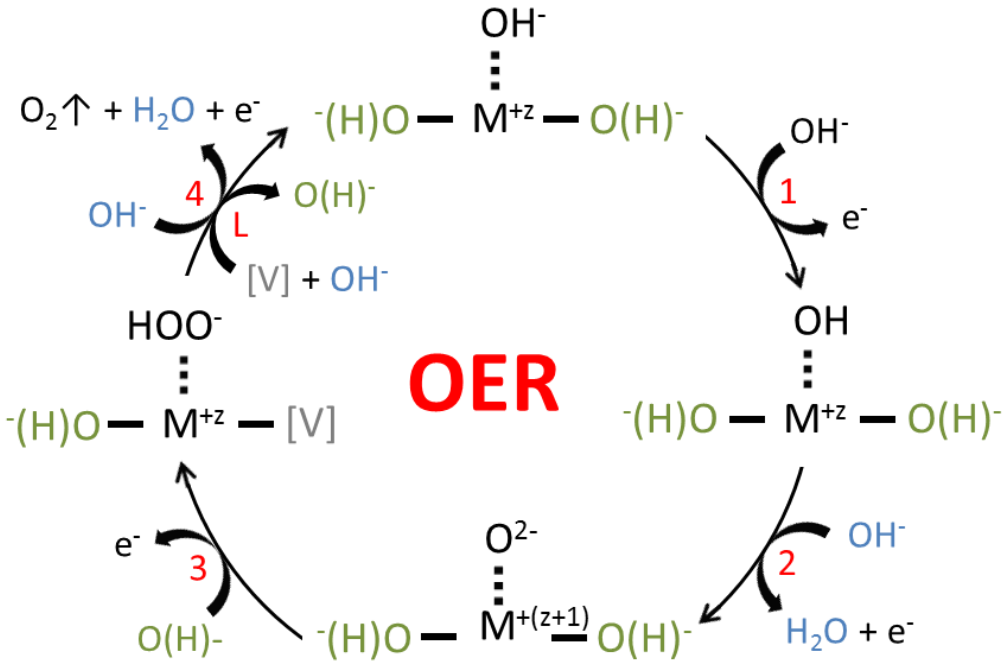

Alkaline OER: $4OH^- \rightarrow O_2 + 2H_2O + 4e^-$

Fierro et al. *Electrochem. Comm.* **2007**
Hardin, Mefford, KPJ, KJS et al., *J. Phys. Chem. Letters* **2013**, Chem. Mater. **2014**

Catalyst Design Principles

More d electrons → greater activity

- More electronegative TM brings 3d electron energies down
- More covalent M – O bond

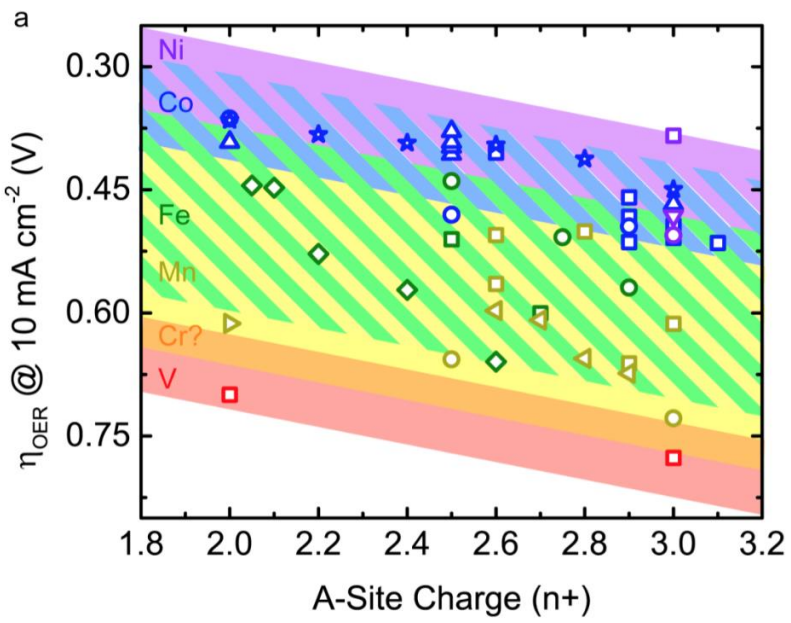

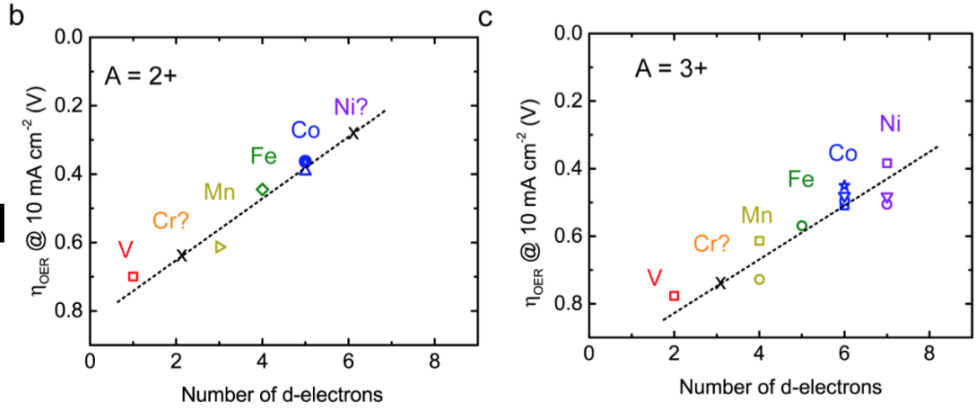

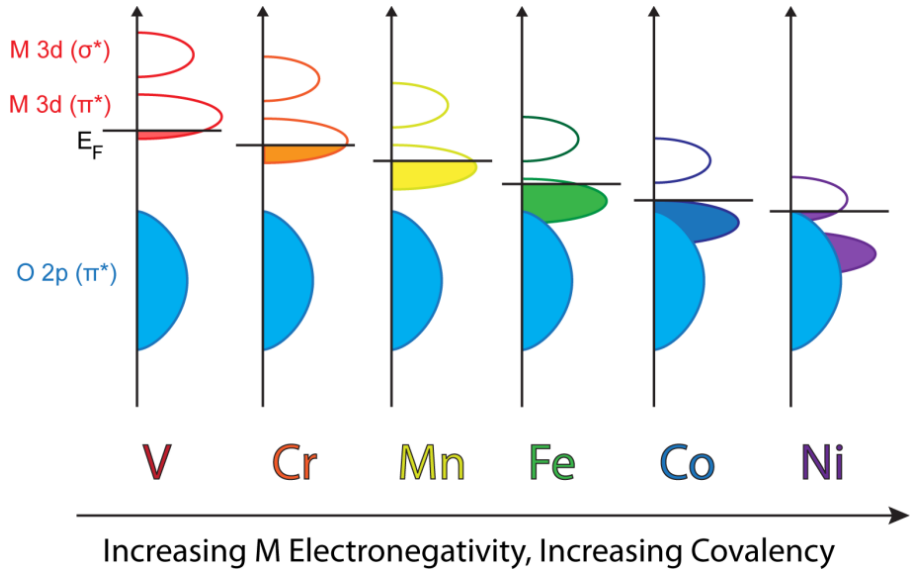

Dr. Kolpak's work on La perovskites and $LaNiO_3$

Rong, Kolpak, *ACS Catalysis* **2016**
Mefford et al. *Nature Comm.*, **2016**

Covalency as a descriptor

How do we test covalency as a descriptor without changing B-sites?

How do we probe lattice oxygen in the OER mechanism?

$La_{1-x}Sr_xCoO_{3-\delta}$

Modulation of Co oxidation state via Charge compensation

- Substitution of La^{3+} for Sr^{2+} increases Co oxidation state
- Mobile lattice oxygen
- Also results in oxygen vacancies

Characterization

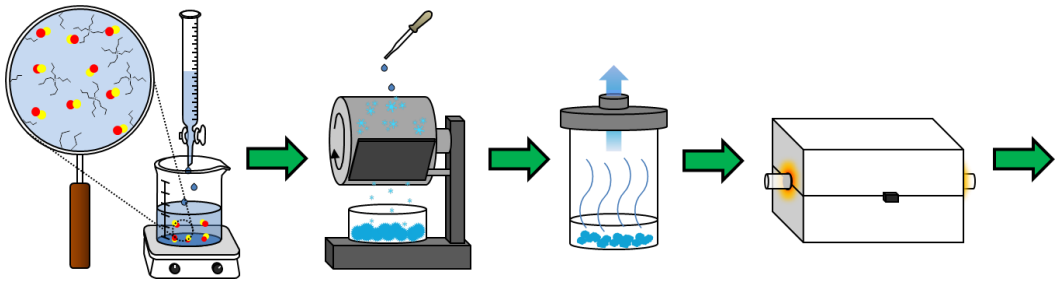

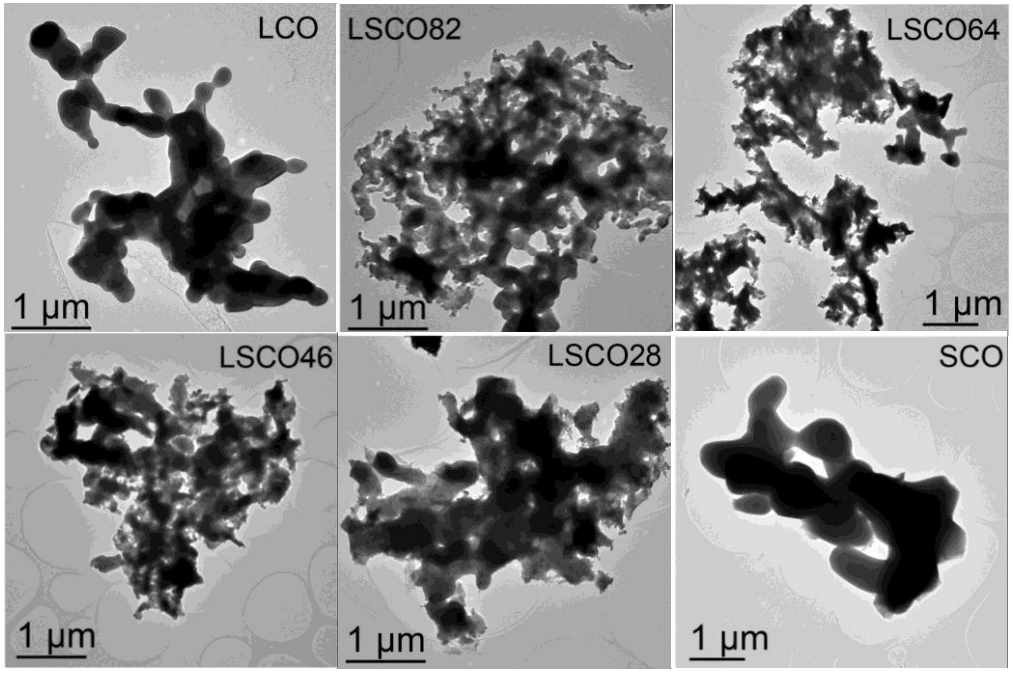

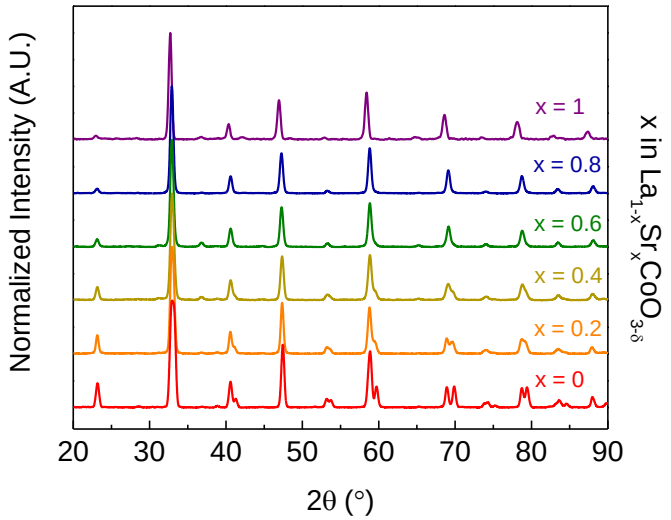

Need similar morphologies, phase purity

$La_{1-x}Sr_xCoO_{3-\delta}$	BET Surface Area ($m^2\ g^{-1}$)
LCO	4.0
LSCO82	4.5
LSCO64	4.2
LSCO46	4.3
LSCO28	3.1
SCO	3.6

Mefford et al. *Nature Comm.* **2016**

OER Activity

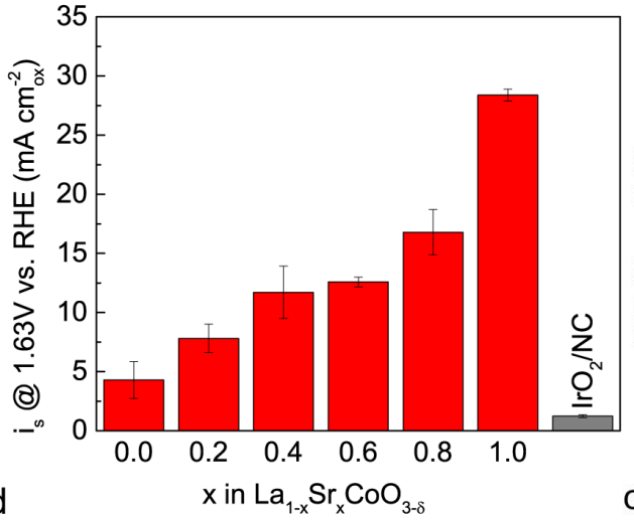

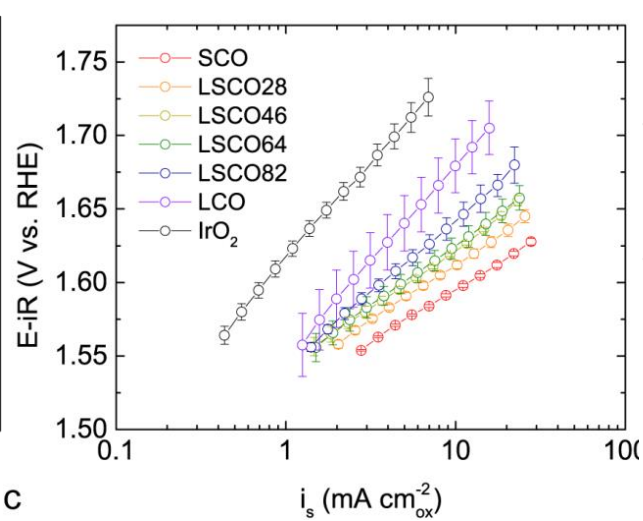

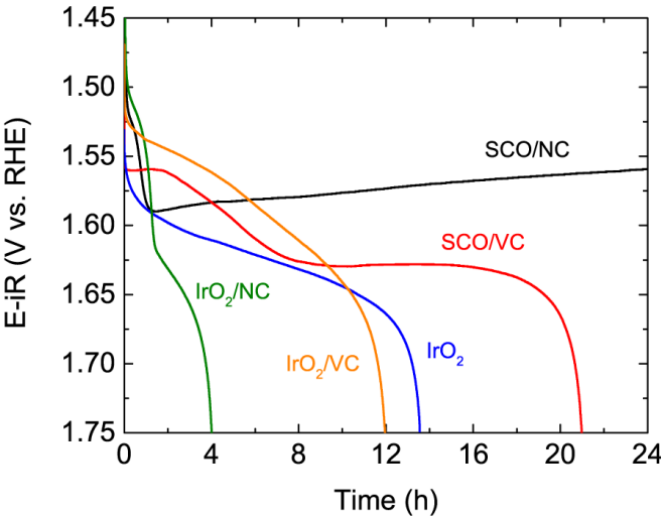

- Fully substituted **$SrCoO_3$** is the **most active,** has lowest taffel slope of 31 mV dec^{-1}
- $SrCoO_3$ on N-doped carbon is the only stable composite over 24 hours

OER conditions: O_2 saturated 0.1 M KOH at 10 mV/s and 1600 rpm; 51 $\mu g_{tot}/cm^2$, 30 wt. % oxide on VC

Mefford et al. *Nature Comm.* **2016**

Oxygen vacancies

- Sr substitution shifts E_F down relative to the 3*d* and 2*p*
- Covalent mixing of orbitals means oxidation and vacancy formation
- Vacancies cause reduction of 3*d*, pinning E_F

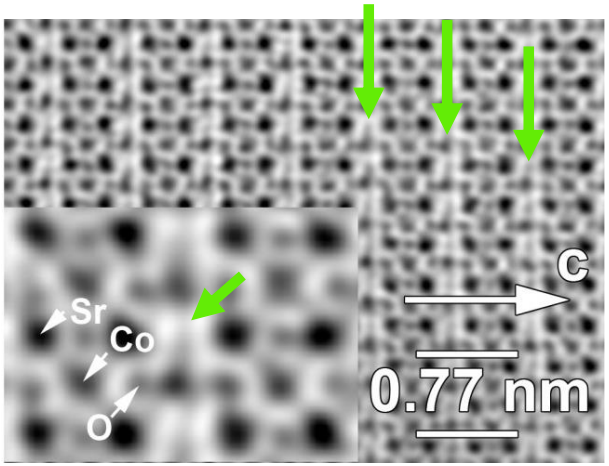

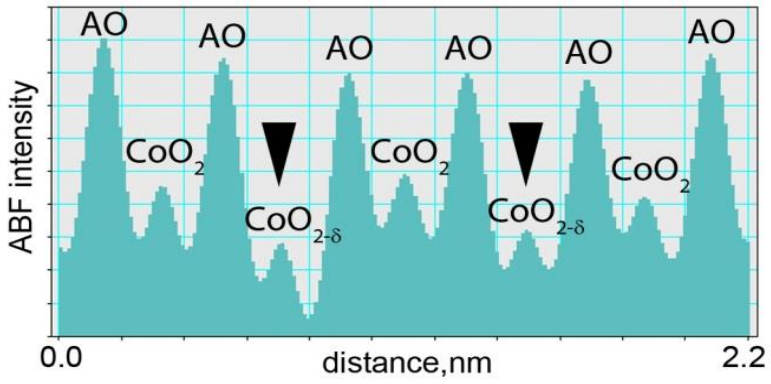

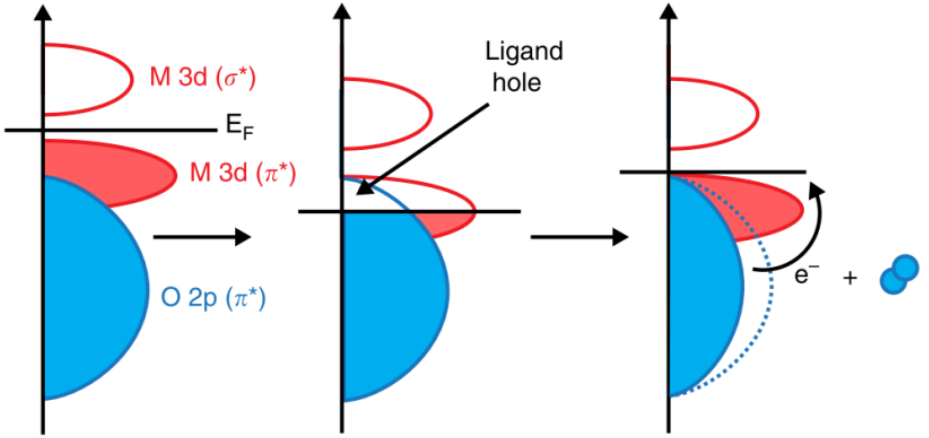

Table 1 | Oxygen vacancy concentration, δ, and cobalt oxidation state, *y*.

x in $La_{1-x}Sr_xCoO_{3-\delta}$	δ	*y*
0	-0.01 ± 0.01	3.01 ± 0.01
0.2	0.01 ± 0.01	3.18 ± 0.02
0.4	0.05 ± 0.04	3.30 ± 0.08
0.6	0.09 ± 0.01	3.43 ± 0.01
0.8	0.16 ± 0.01	3.48 ± 0.02
1.0	0.30 ± 0.03	3.40 ± 0.06

Error is based on the s.d. of triplicate measurements.

Mefford et al. *Nature Comm.* **2016**

Vacancy mediated oxygen intercalation

Vacancies are mobile, can act as sites for insertion/removal of electrolyte oxygen species

- Insertion/removal can be controlled electrochemically
- O^{2-} diffusion rates range between 10^{-14} to 10^{-12} cm^2/s for LSCO series
- Vacancies increase the diffusion rate exponentially

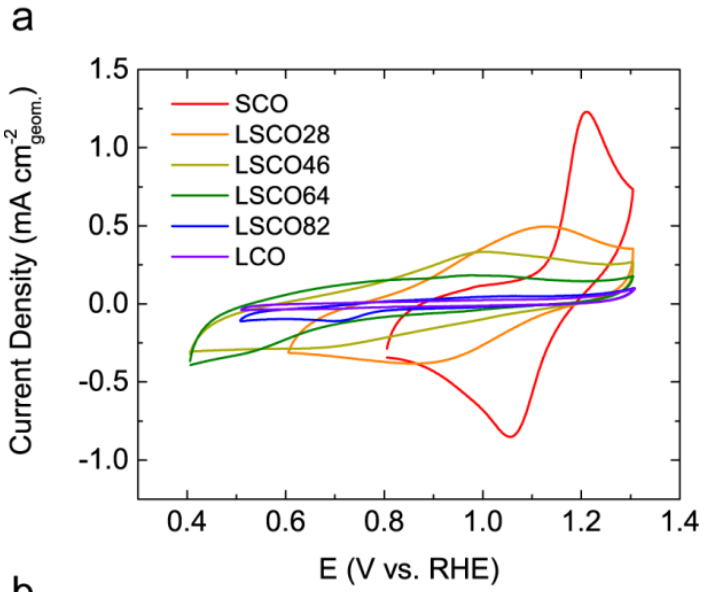

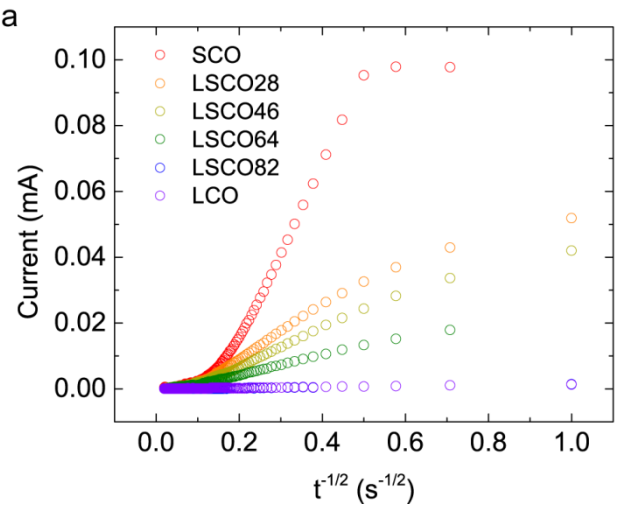

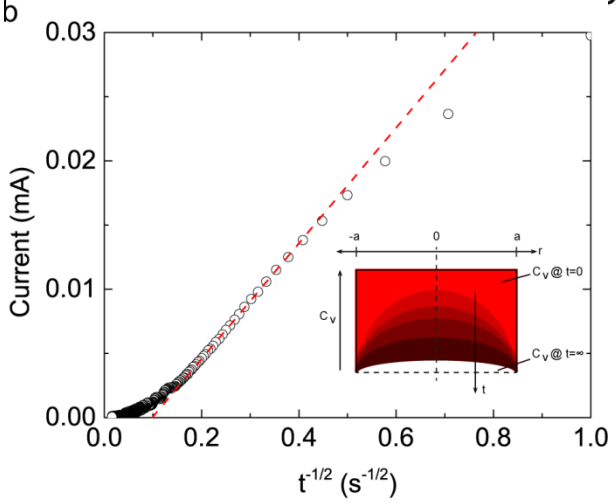

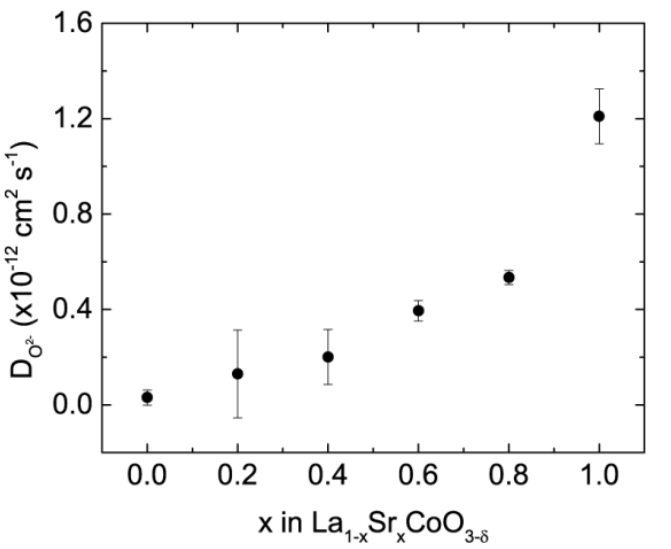

Mefford et al. *Nature Comm.* **2016**

Lattice Oxygen Mediated OER

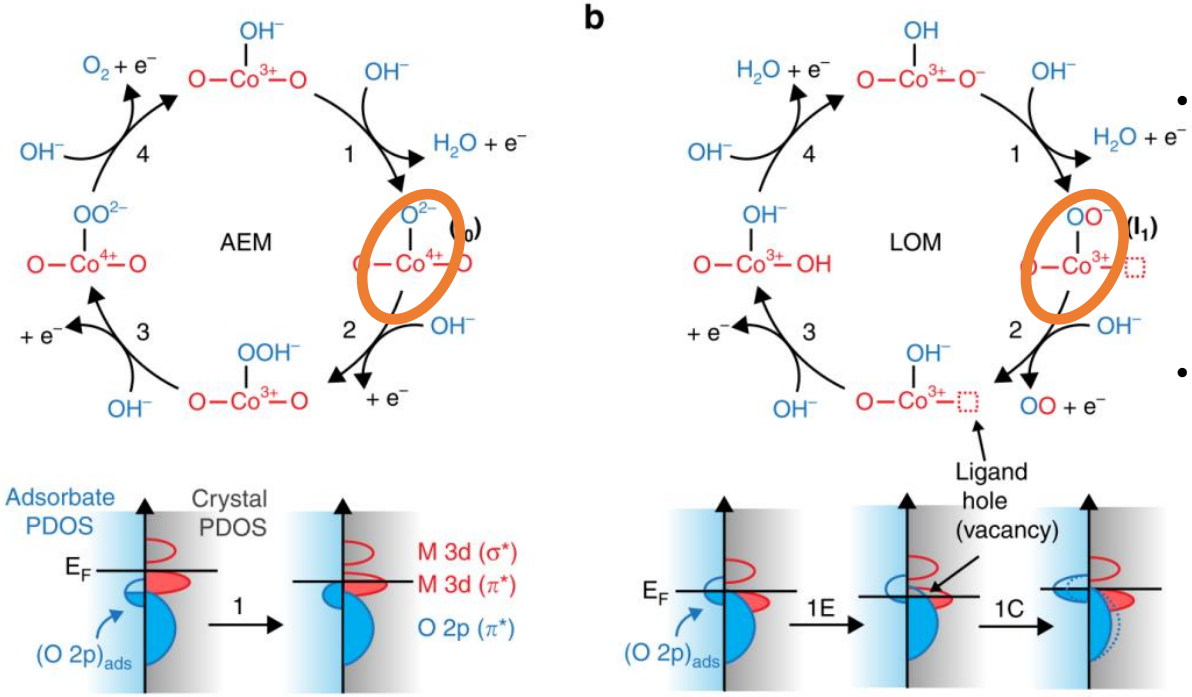

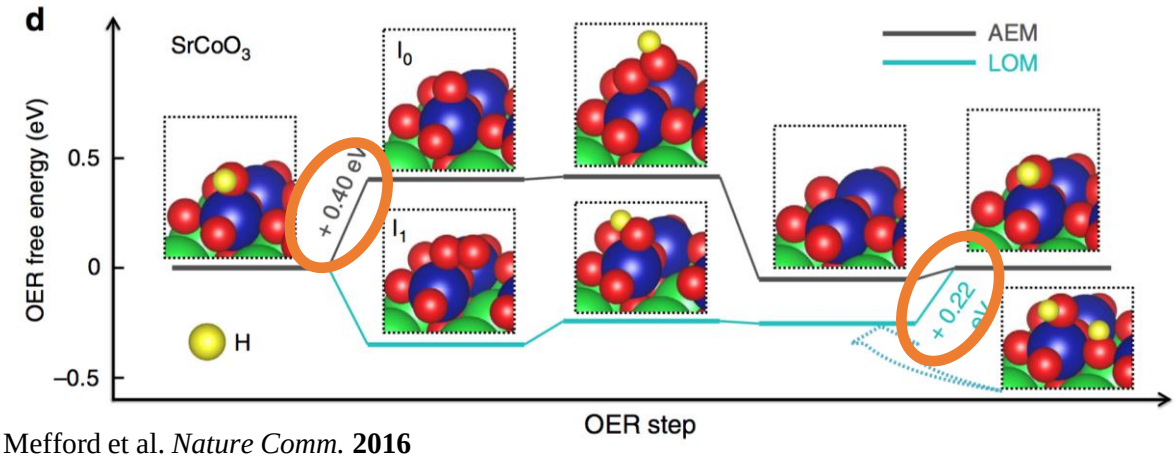

- New OER mechanism proposed, supported by DFT → lattice oxygen mediated (LOM)
  - Lower ΔG for RDS
  - Requires M-O bond covalency
- Labile lattice oxygen experimentally shown as indicator of M-O covalency

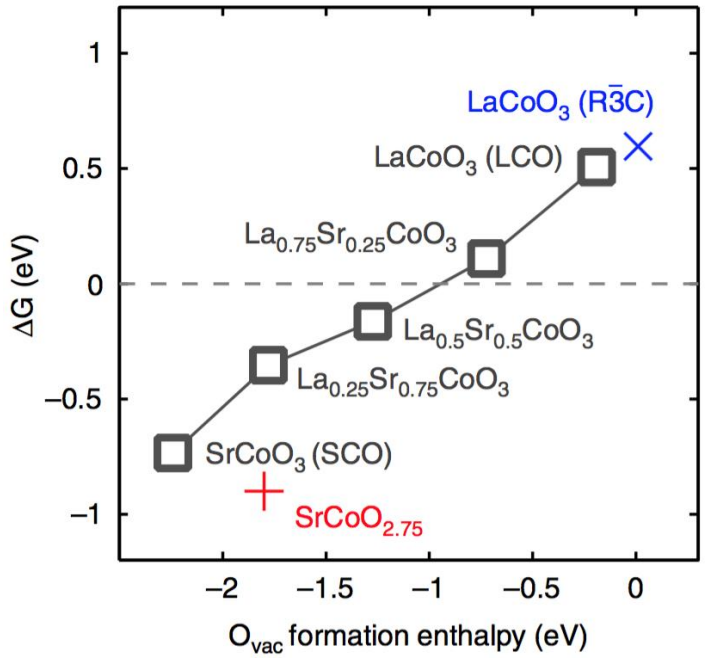

Mefford et al. *Nature Comm.* **2016**

LOM Mechanism Verification

Shao Horn group later used isotopic labeling of lattice oxygen to confirm an LOM mechanism was taking place

- Only $La_{0.5}Sr_{0.5}CoO_3$ and $SrCoO_3$ showed evolved oxygen from the lattice
- pH dependence of OER activity only for 50% and full Sr substitution → mechanism shift

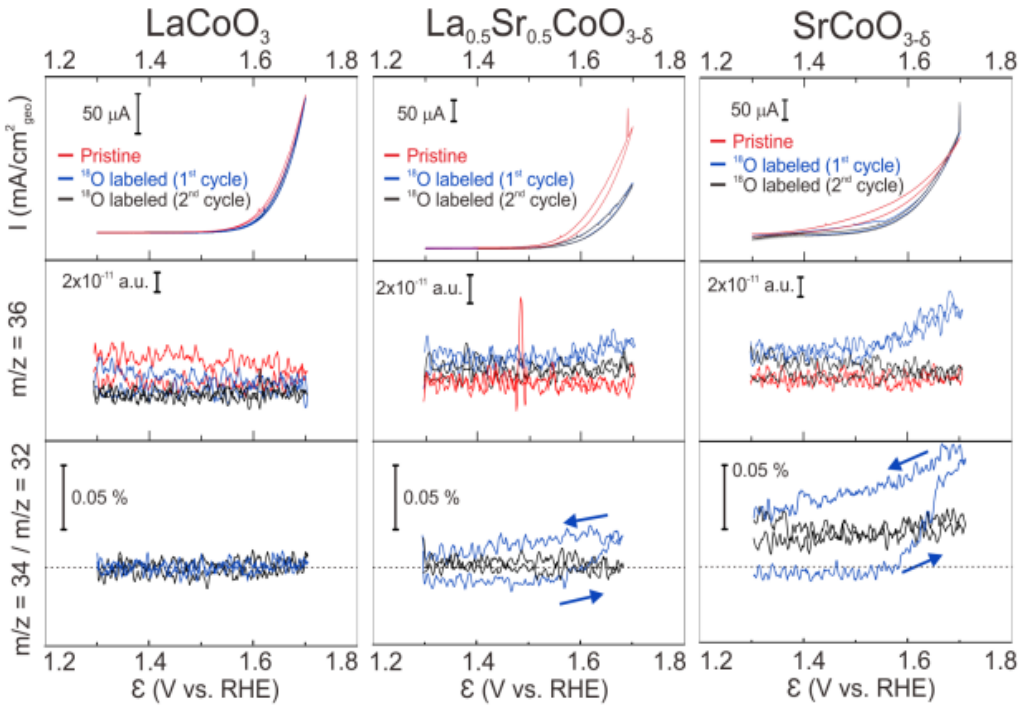

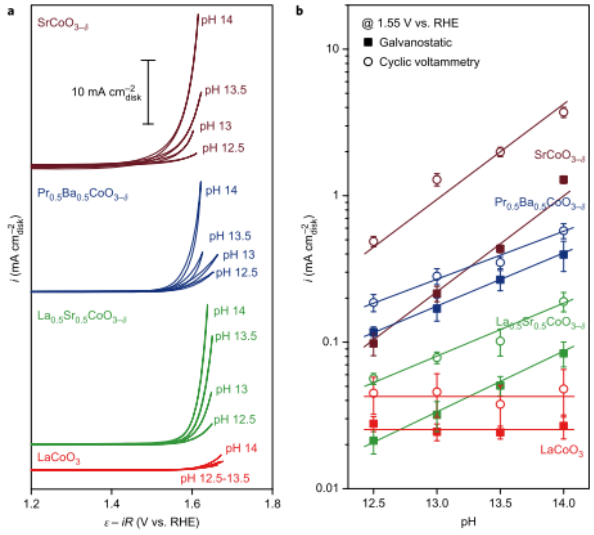

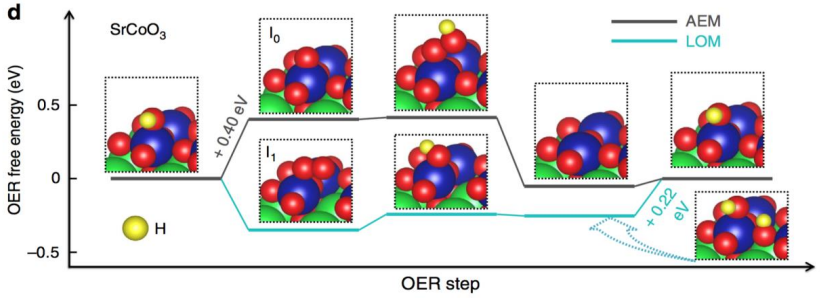

Grimaud et al. *Nature Chem.* **2017**
Mefford et al. *Nature Comm.* **2016**

Experimental evidence of LOM OER

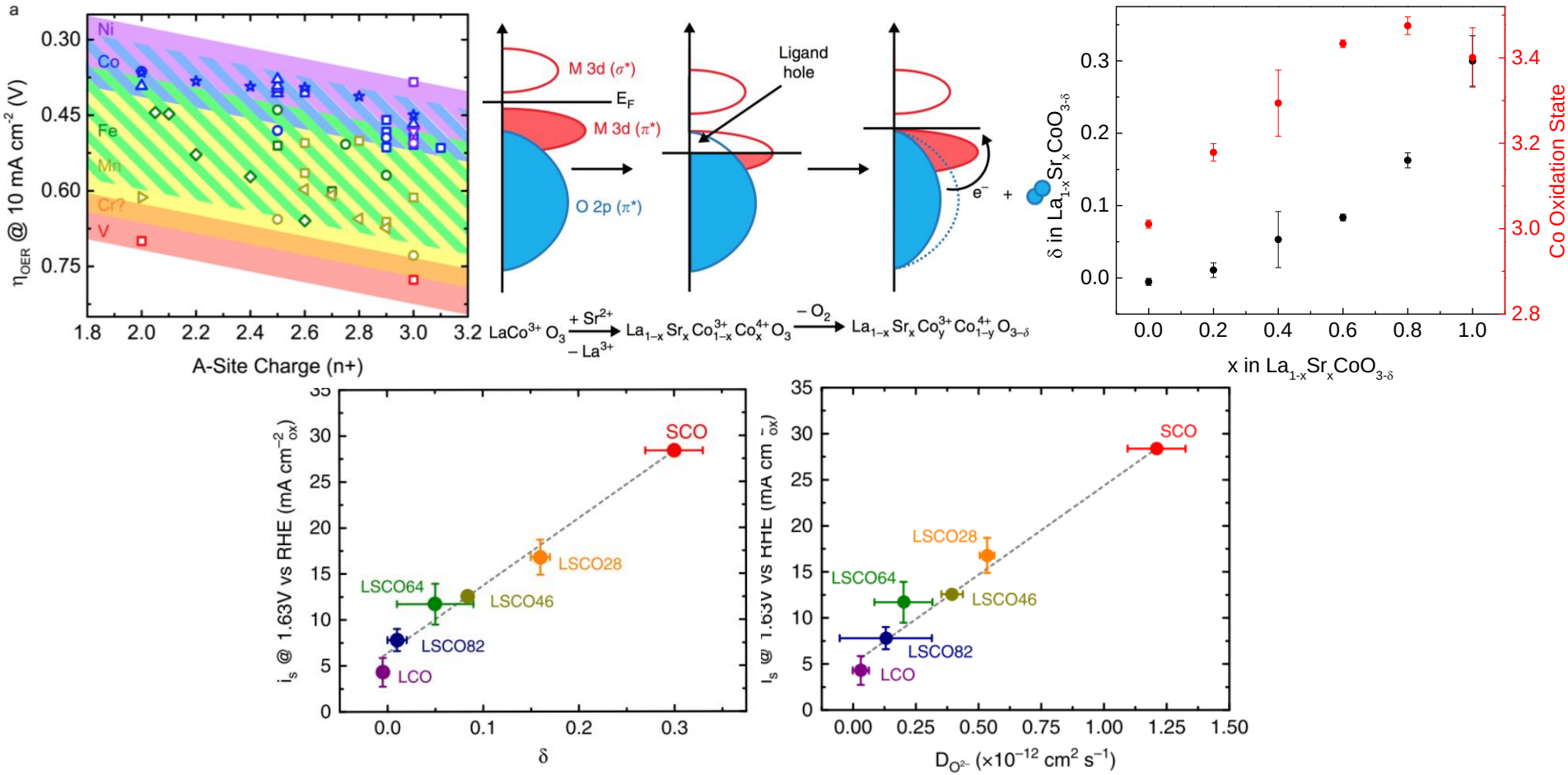

Experimentally show M – O bond covalency, oxygen vacancies, oxygen diffusion, OER activity **all tied together**

Mefford et al. *Nature Comm.* **2016**

DFT evidence of LOM OER

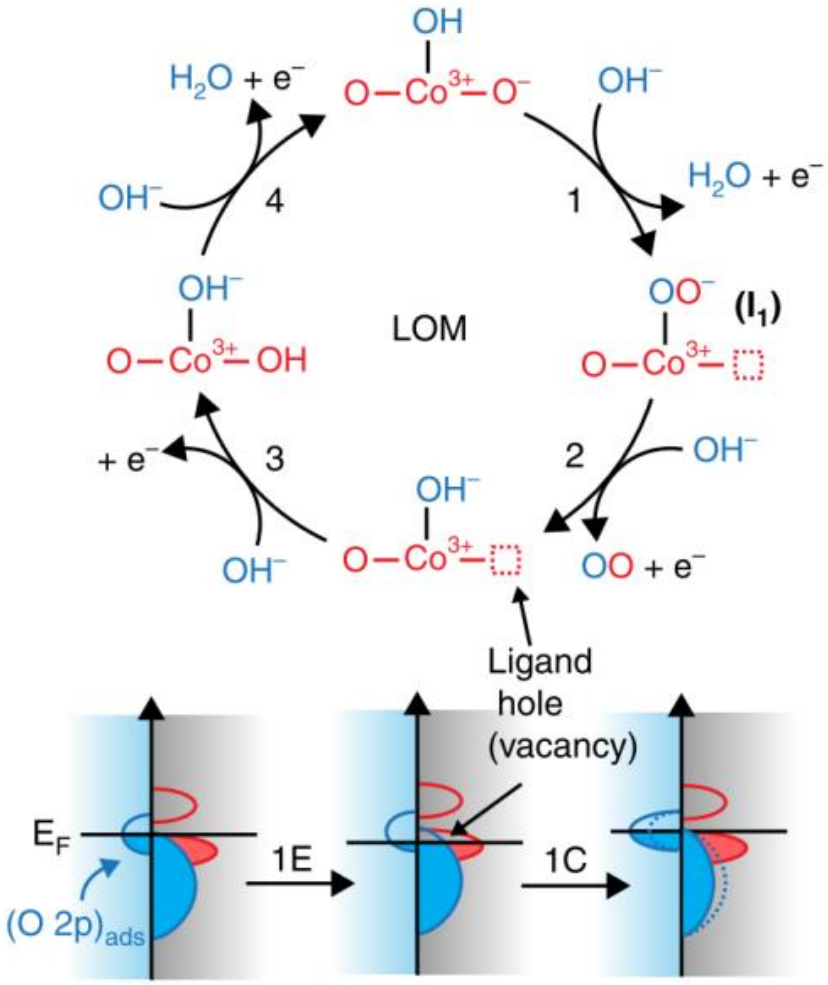

New OER mechanism proposed

- DFT → lattice oxygen mediated (LOM) mechanism
- Lower ΔG for RDS
- Requires M-O bond covalency

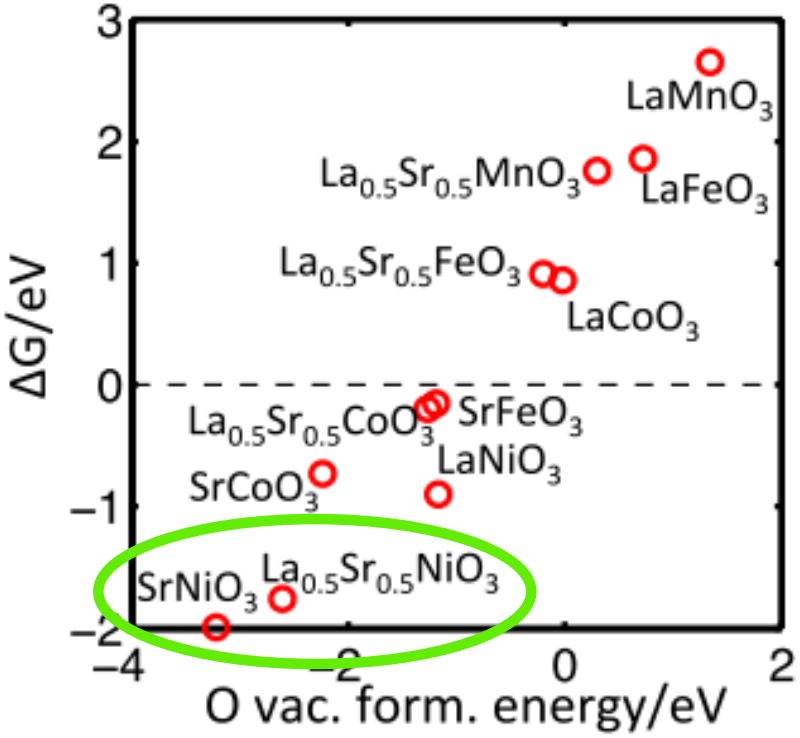

$SrNiO_3$ predicted to be the best OER catalyst

Mefford et al. *Nature Comm.* **2016**

Ni–Fe interactions

Fe incorporation into NiOOH dramatically increases OER activity

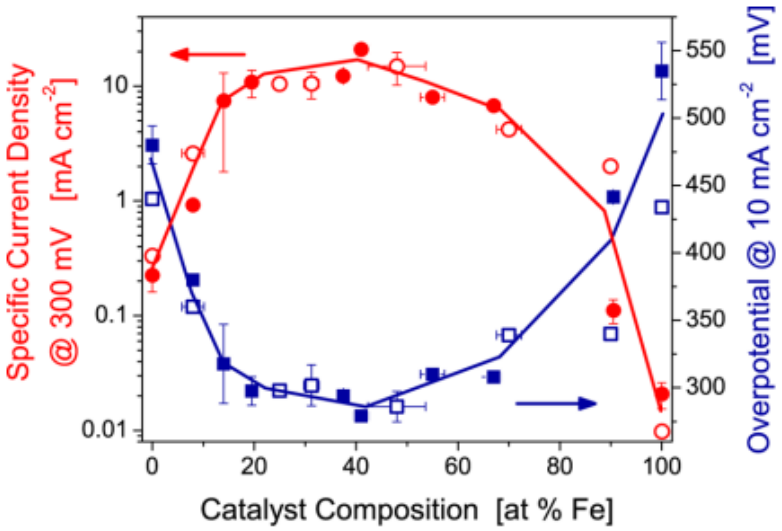

Louie, Bell *et al* JACS 2013

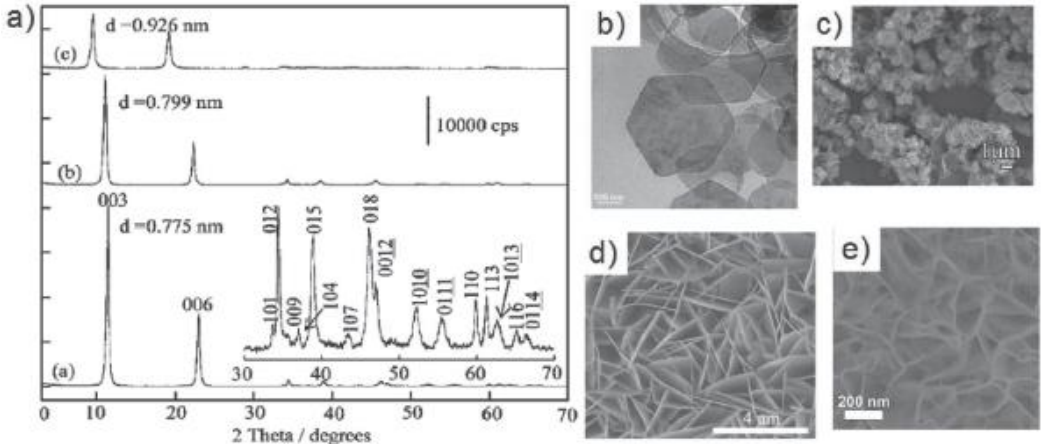

Dionigi, Strasser *et al* Adv. Energy Mater. 2016

Structural variations, poor crystallinity complicate structure-property relationship

How to incorporate mechanistic insights from perovskites (M-O covalency), predicted materials ($SrNiO_3$) and Ni-Fe interactions into a crystalline catalyst system that supports the establishment of structure-property relationships?

$SrNi_{1-x}Fe_xO_3$?

$SrNiO_3$ not thermodynamically stable!

MATERIALS CHEMISTRY COMMUNICATIONS

Preliminary Crystal Structure of Mixed-valency $Sr_4Ni_3O_9$, the Actual Formula of the so-called $Sr_5Ni_4O_{11}$

Francis Abraham,* Sylvie Minaud and Catherine Renard
Laboratoire de Cristallochimie et Physicochimie du Solide, URA CNRS 0452, ENSCL, Université des Sciences et Technologies de Lille, B.P. 108, 59652 Villeneuve d'Ascq Cedex, France

A crystal structure investigation of the so-called $Sr_5Ni_4O_{11}$ from single-crystal X-ray data has shown that the composition of this oxide is in fact close to $Sr_4Ni_3O_9$. The structure has been solved in the trigonal *P*321 space group. The final refinement gave an *R* factor of 0.045 for 512 independent reflections. The structure contains NiO_3 chains with two NiO_6 octahedra and one NiO_6 trigonal prism alternating and sharing faces. The chains run along the three-fold axis and are connected by Sr ions. The Ni—O distances seem to indicate a possible repartition of Ni^{IV} in the octahedral sites and Ni^{II} in the trigonal pris

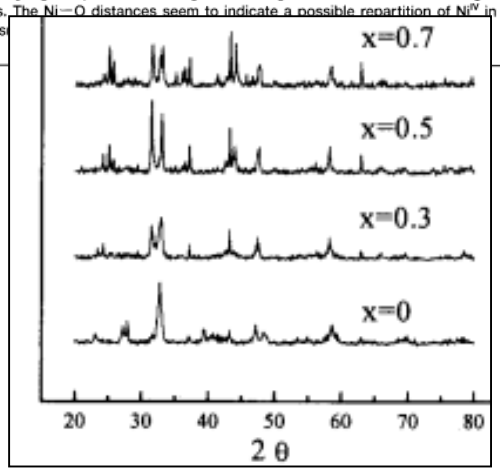

SYNTHESIS OF $SrNiO_3$ AND RELATED COMPOUND, $Sr_2Ni_2O_5$

Y. TAKEDA, T. HASHINO,* H. MIYAMOTO,† F. KANAMARU, S. KUME and M. KOIZUMI
The Institute of Scientific and Industrial Research, Osaka University, Suita, Osaka, Japan

(*Received* 6 *August* 1971)

Abstract—Two crystal phases of strontium-nickel oxides, $SrNiO_3$ and compounds with composition near $Sr_2Ni_2O_5$, containing tetra- and tri-valent nickel ions respectively, have been synthesized in oxidation atmosphere. $SrNiO_3$ synthesized under high pressures of oxygen above 50 atm has a hexagonal unit cell with $a = 5{\cdot}355 \pm 0{\cdot}001$, $c = 4{\cdot}860 \pm 0{\cdot}001$A and is isostructural with $BaNiO_3$ with perovskite-like structure. The phase with composition near $Sr_2Ni_2O_5$ with hexagonal unit cell has been synthesized above 600°C and at 1 atm of wet oxygen gas. The existence of water has a remarkable effect to form both the compounds of $SrNiO_3$ and $Sr_2Ni_2O_5$.

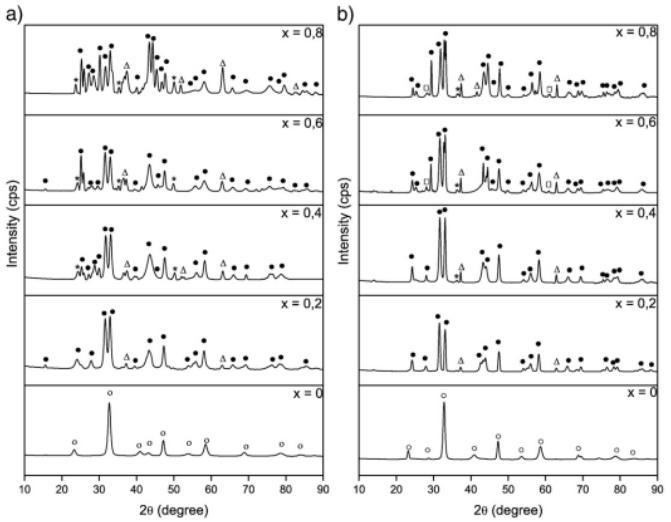

Fig. 2. XRD of $La_{1-x}Sr_xNiO_3$ ($0 \le x \le 0.8$) systems calcined at a) 700 °C and b) 900 °C. Symbols: ○ = $LaNiO_3$; ● = $La_{1-x}Sr_xNiO_3$; Δ = La_2O_3; * = NiO; □ = $SrNiO_3$.

How do we get Sr and Ni in the same material?

Ruddlesden-Popper

Ruddlesden-popper: $(AO)(ABO_3)_n$

- ***n* represents the number of perovskite layers** (ABO_3) separated by a rock-salt (AO) interface
- As **n** → ∞, RP becomes pure ABO_3 perovskite
- AO-ABO_3 interface accommodates ions that would be too large for pure perovskite: RP supports structural (and electronic) configurations **not realizable in perovskites**

Average oxidation state of B site in $(AO)(ABO_3)_n$ is controlled by A and B's valence, B's electronegativity, and *n*

n	Formula	A = Ln^{3+}, B^{x+}	A= Sr^{2+}, B^{x+}
1	$A_2BO_{4\pm\delta}$	2	4
…	$(AO)(ABO_3)_n$	> 2.66	4
∞	ABO_3	3	4

Location of strained AO interfaces that support Sr^{2+} substitution of La^{3+} which is unstable in a pure perovskite phase

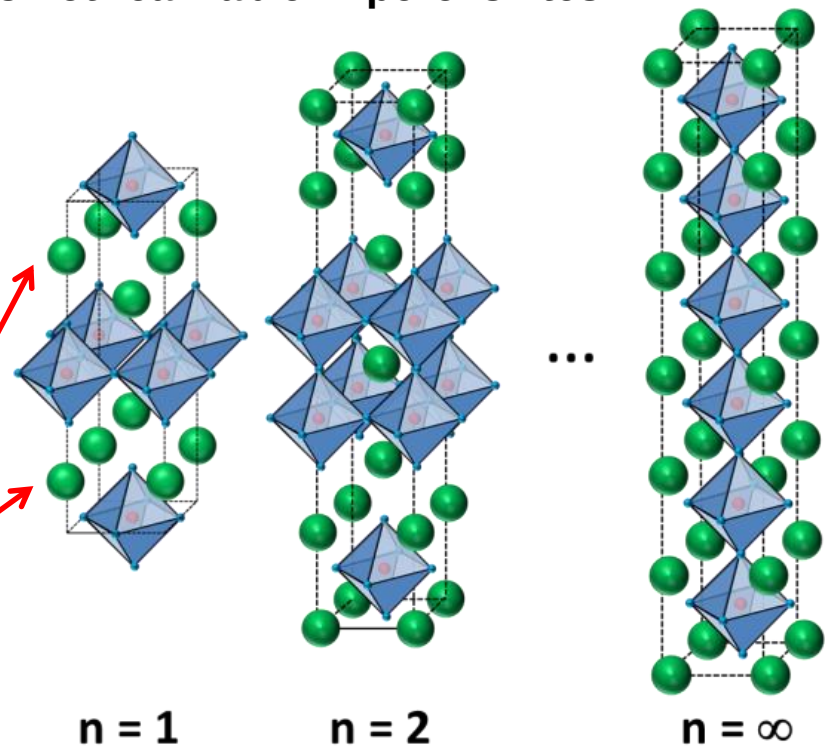

New synthesis for RP Catalysts

Pechini Method:

A. Complexation of metal nitrates by **citric acid and EDTA** in water
   Titration with TMAOH to raise pH to ~7 to deprotonate EDTA

B. Addition of DEG followed by heating to 80°C
   Condensation reaction driven by the evaporation of water forms polyester gel with metal cations intermixed

C. Combustion at 300°C to form mixed metal oxide foam

D. Calcination at temperatures above 950°C to form the RP phase

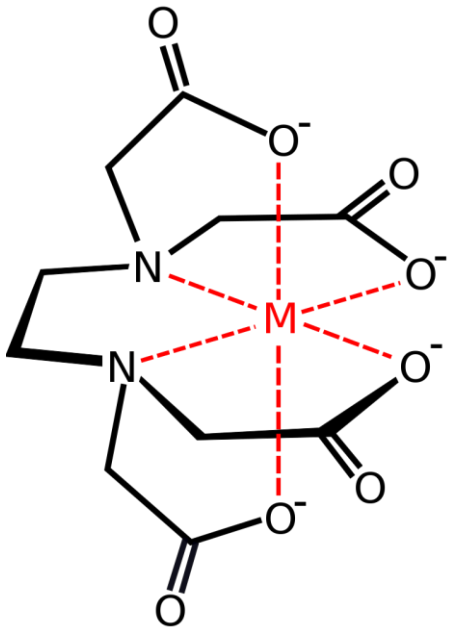

Yield increased 20x

Took 1 day vs. almost 2 weeks

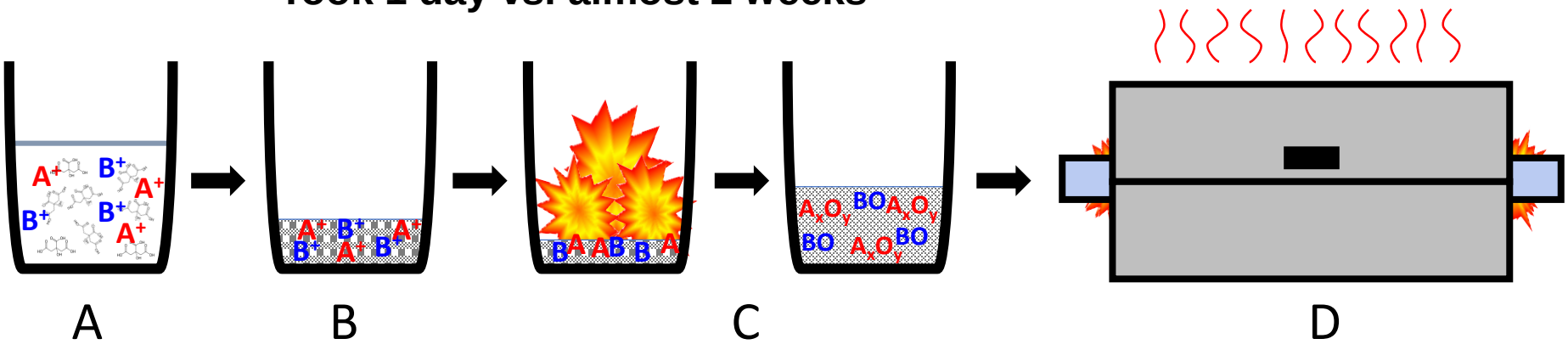

Forslund, Hardin, et al. *under review* **2017**

$La_{0.5}Sr_{1.5}Ni_{1-x}Fe_xO_{4+\delta}$

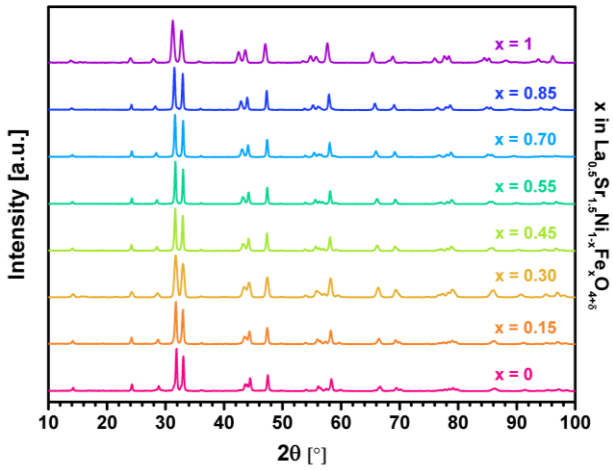

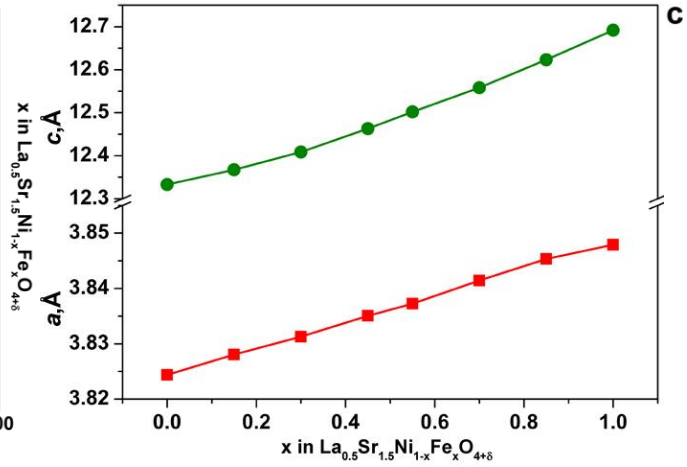

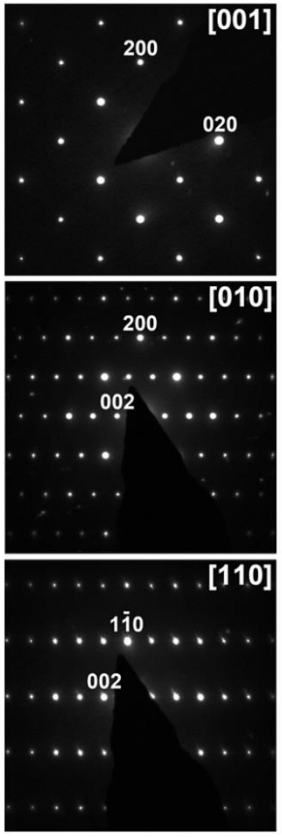

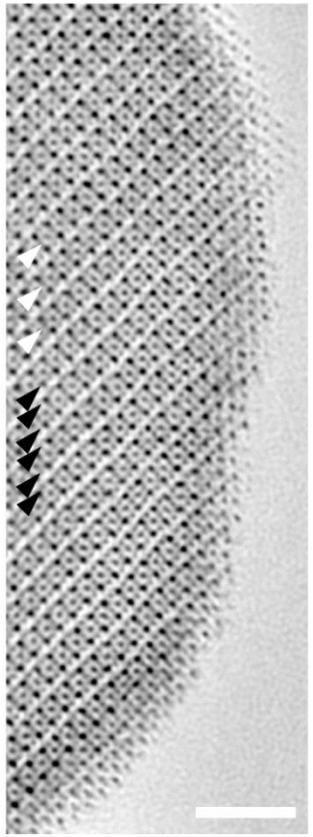

- **25% La and controllable Fe substitution** in *n*=1 $La_{0.5}Sr_{1.5}NiO_4$ Ruddlesden-Popper.
- A-site substitution for La imparts **RT stability** and lowers crystallization temp, B-site substitution for Fe stabilizes high-valence Ni.
- Substitution of Fe for Ni systematically increases unit cell parameters, no ordered oxygen vacancies or interstitials evident by ABF-STEM

Electron diffraction (ED) of multiple zone axes indicates tetragonal *n* = 1 Ruddlesden-Popper *I*4/*mmm* structure

Forslund, Hardin, et al. *under review* **2017**

Characterization

Why we need EDTA

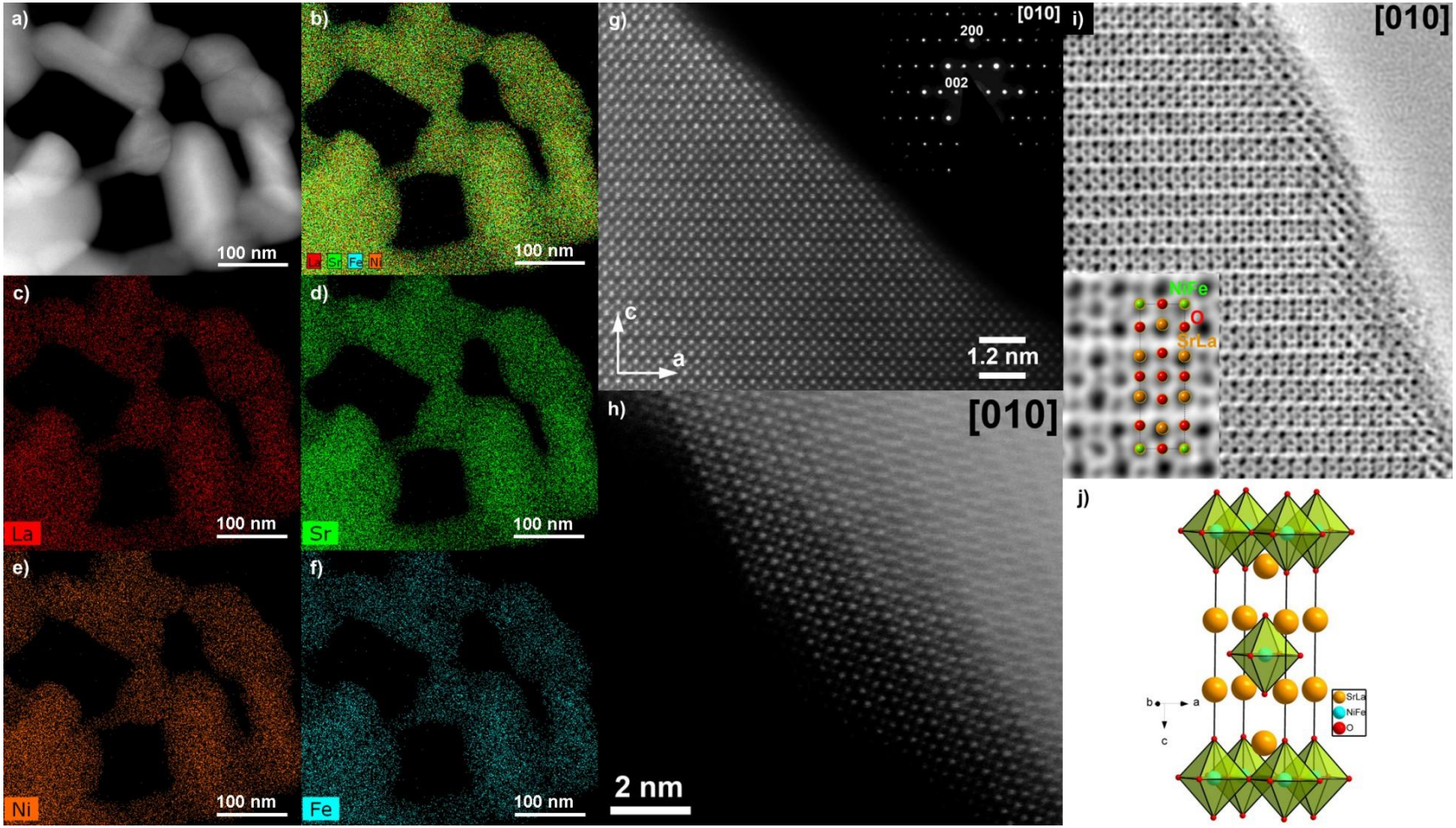

Forslund, Hardin, et al. *under review* **2017**

OER activity

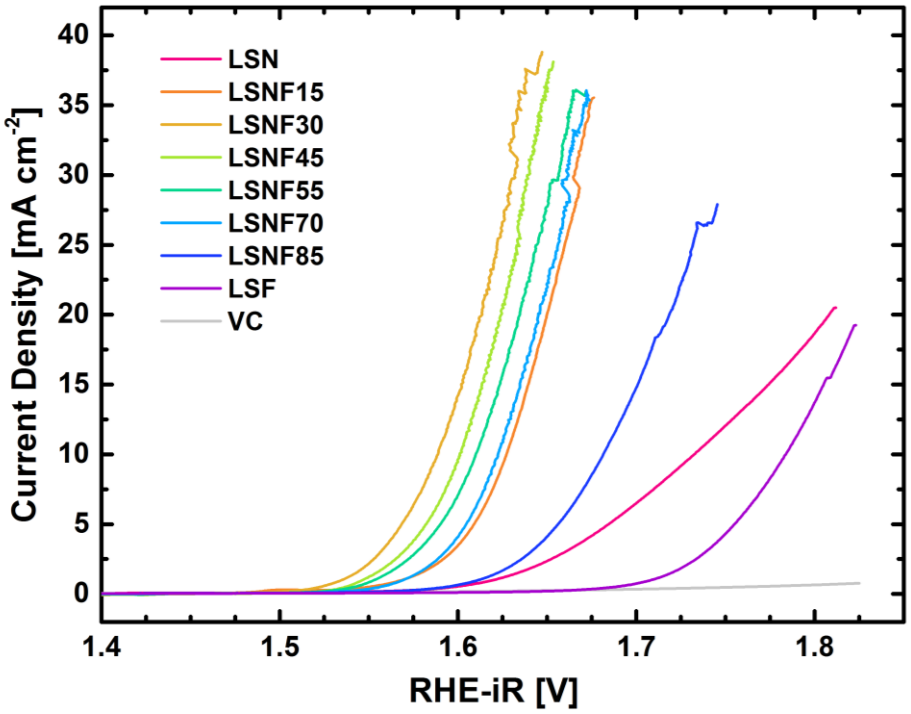

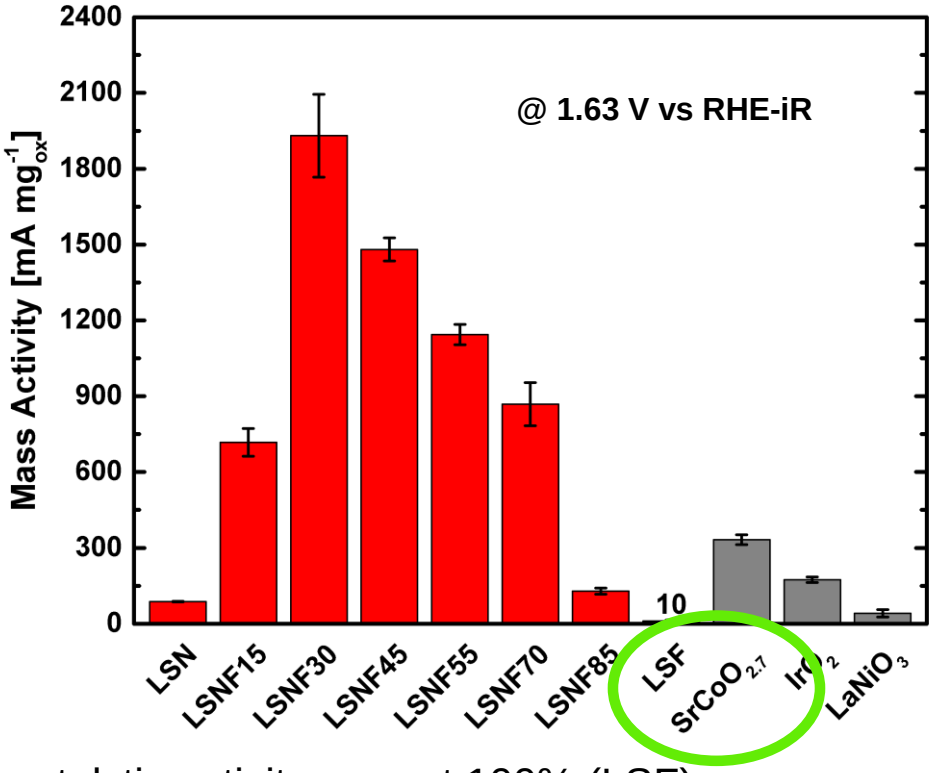

- All amounts of Fe substitution increase catalytic activity, except 100% (LSF)
- Most active composition being LSNF30 (32.7 mA cm^{-2}_{ox})
- Polarization curves are averaged between anodic and cathodic scans to eliminate capacitive effects → **little to no hysteresis indicates catalyst stability**

OER conditions: O_2 saturated 0.1 M KOH at 10 mV/s and 1600 rpm; 51 $\mu g_{tot}/cm^2$, 30 wt. % oxide on VC

Forslund, Hardin, et al. *under review* **2017**

Composite stability

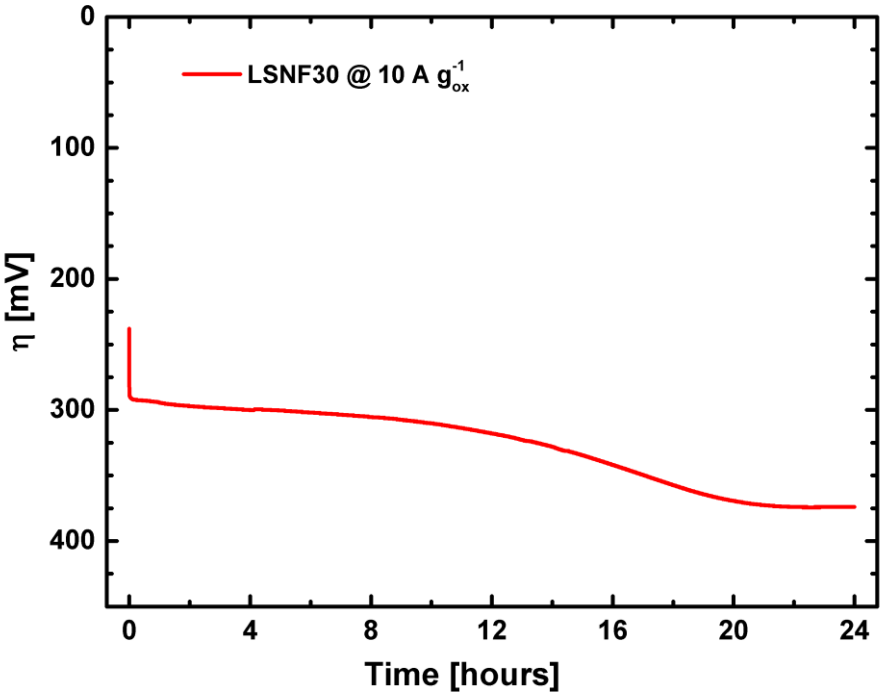

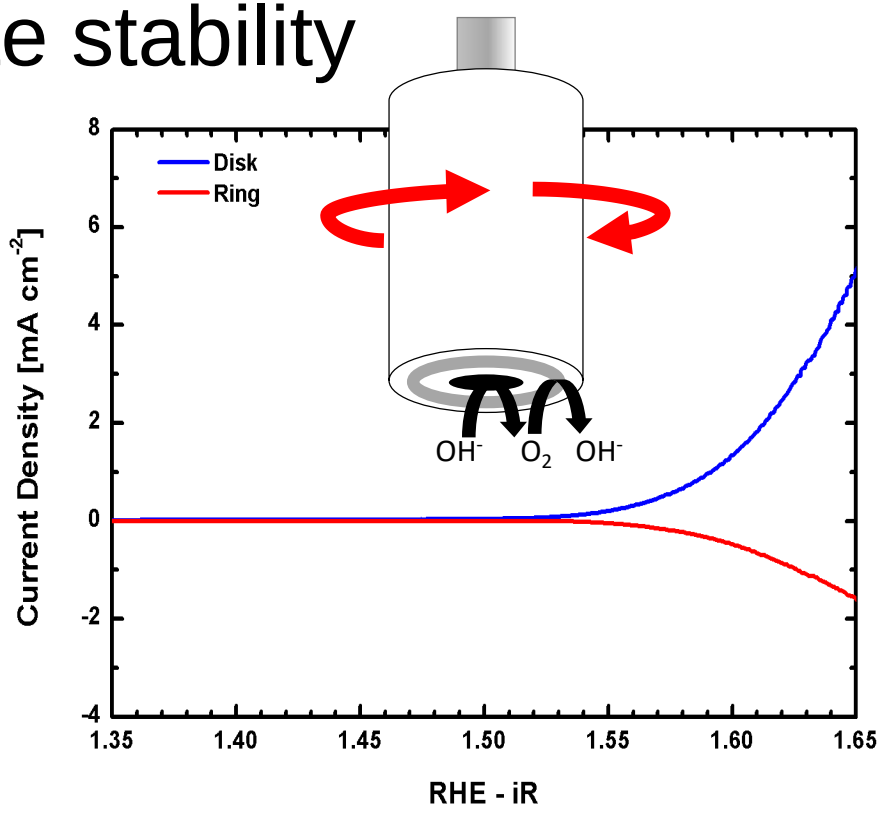

- LSNF30 is stable for over 24 h under galvanostatic (10 A/g_{ox}) stability testing in O_2 saturated 0.1 M KOH and 1600 rpm.
- Only $SrCoO_3$ on N-doped carbon was stable before

- RRDE produces oxygen at the GC disk then reduces it at the Pt ring.
- Performed with ¼ normal mass loading, rotated at 2400 rpm
  - prevent bubble formation that limits collection efficiency.

Ni redox and oxygen intercalation

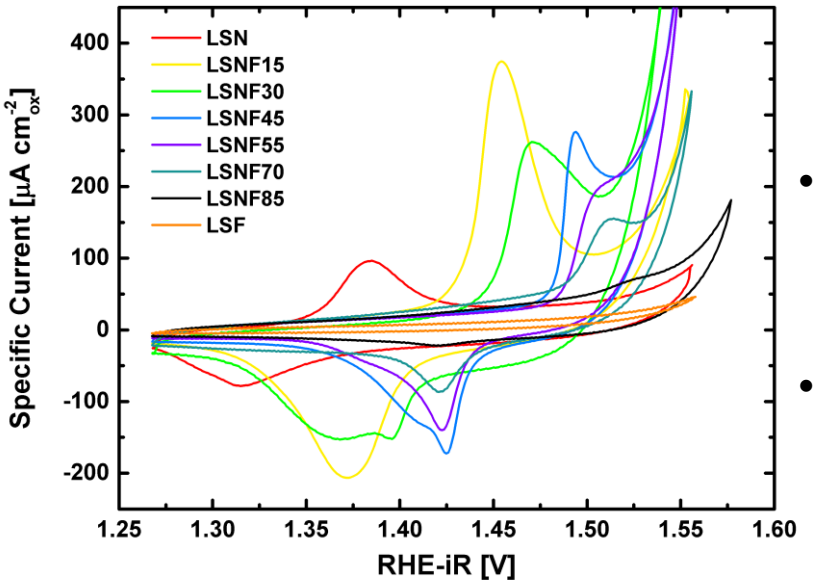

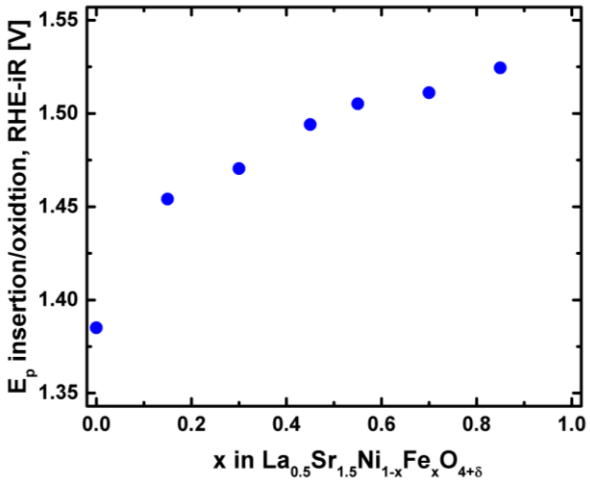

- $Ni^{2+/3+}$ redox features seen in incipient OER region

$$Ni^{2+} \quad Ni^{3+} + e^-$$

- Fe substitution moves the peak potential (E_P) of $Ni^{2+/3+}$ oxidation towards the OER
  - ➢ Indicates modulation of Ni's electronic properties, oxidative strength
- Area under oxidation wave consistently decreases w/ increasing Fe sub, with the exception of LSNF15
- Hydroxide ion intercalation occurring simultaneously?

Forslund, Hardin, et al. *under review* **2017**

Oxygen diffusion in LSNF

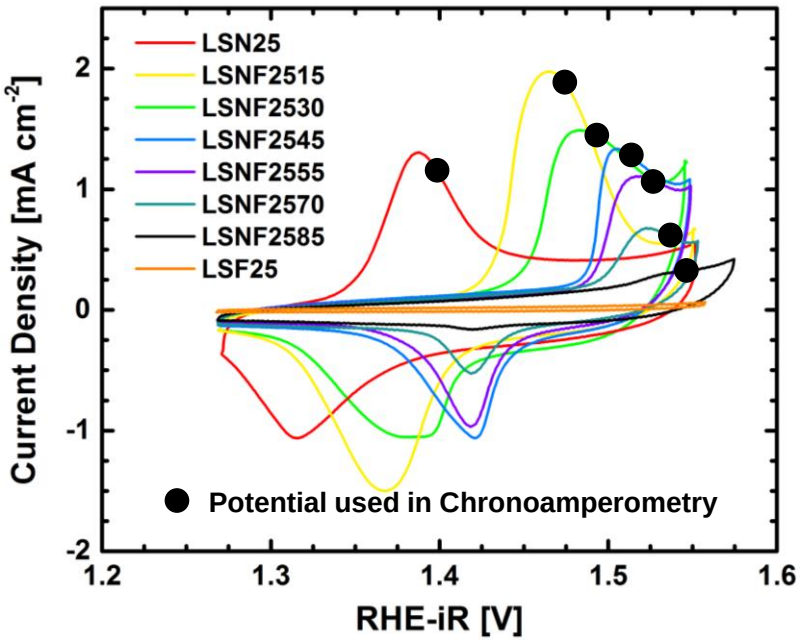

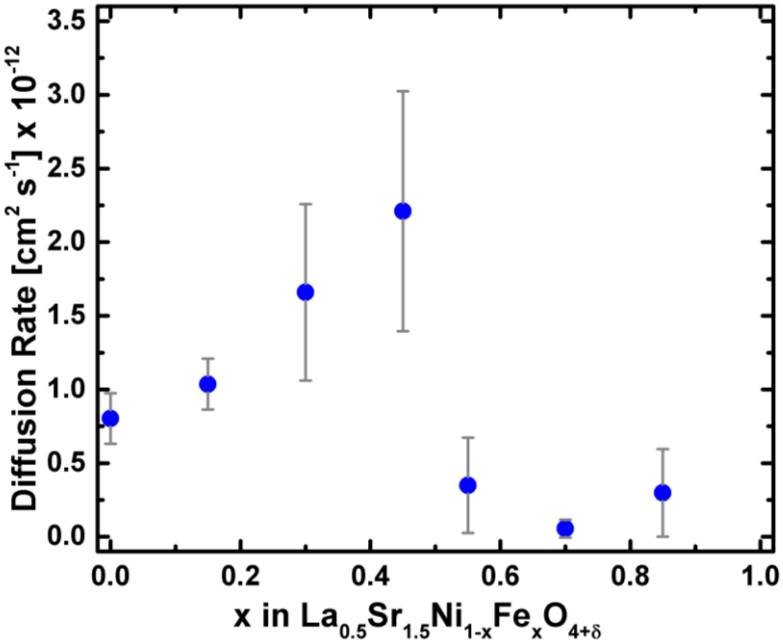

- Bounded 3D diffusion model used to calculate diffusion rates, all tests done in triplicate
- Oxygen diffusion rate of LSNF45 is 2 x 10^{-12} cm^2/s**,** comparable to Li^+ in Li-ion batteries
- Hydroxide ion intercalation concomitant with Ni $^{2+/3+}$ redox supported
  - ➢ Mobile lattice oxygen supports the LOM OER mechanism!

Chronoamperometry in O_2 saturated 1 M KOH. Potentials were chosen 10 mV anodic of E_p to **measure diff. limited intercalation**

Mössbauer spectroscopy

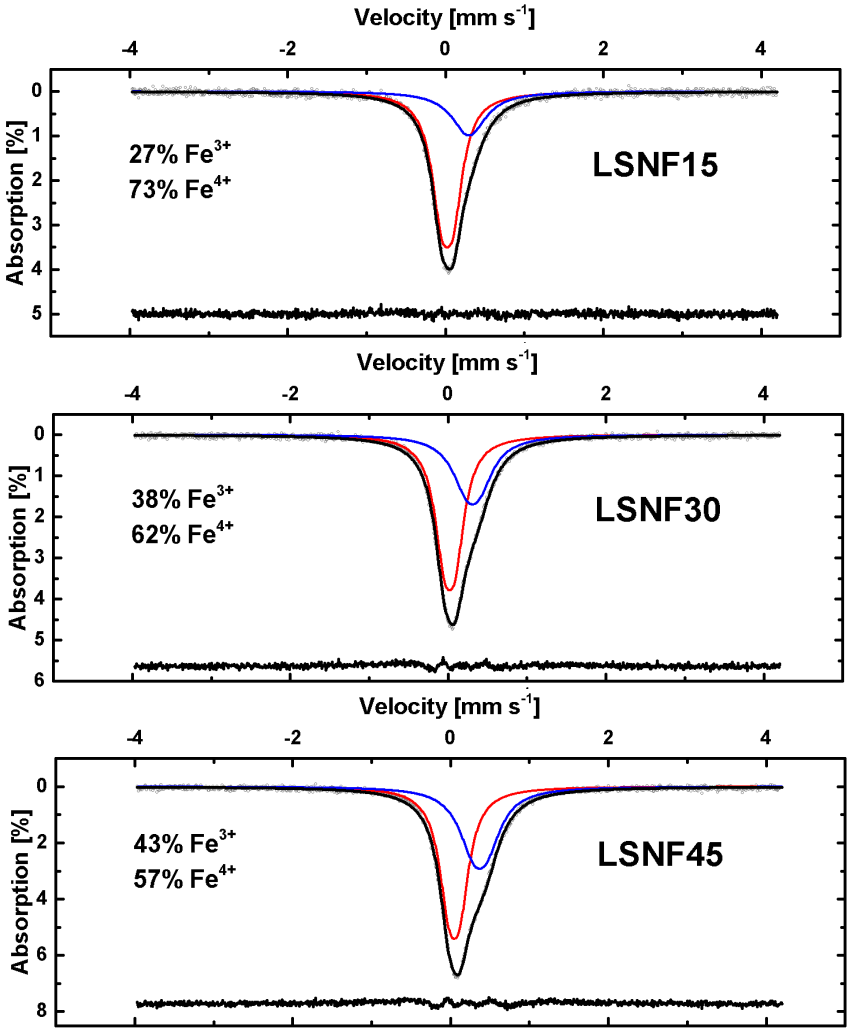

Can use Mössbauer in conjunction with iodometric titrations to find the oxidation state of Ni

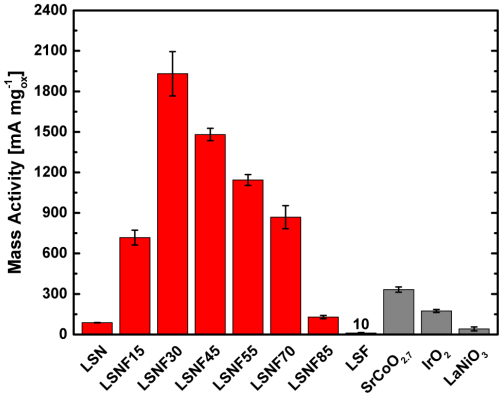

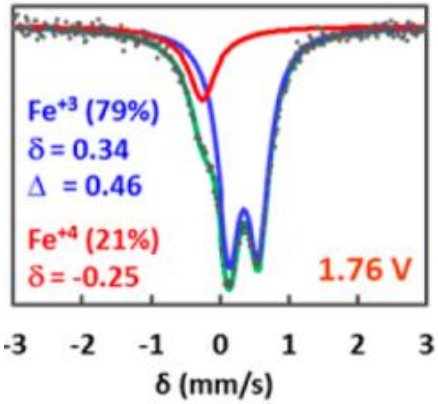

- Deconvolution of room temp. Mössbauer spectroscopy
- Consistent with detection of Fe^{4+} in Ni-Fe oxyhydroxides by Chen, Stahl *et al.;* JACS 2015

Forslund, Hardin, et al. *under review* **2017**

B-site oxidation states

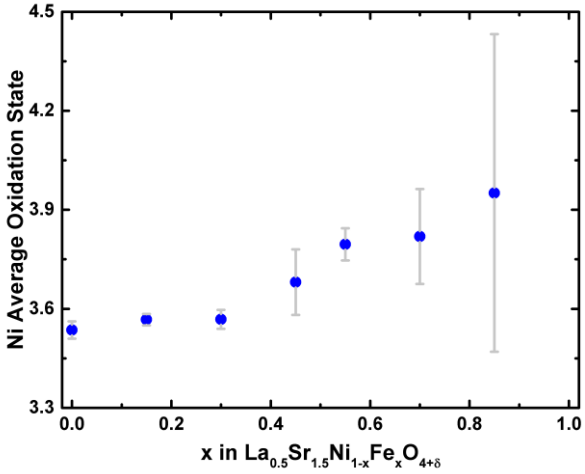

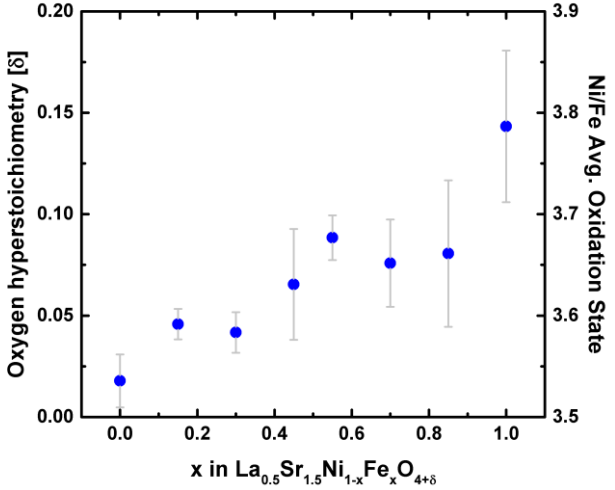

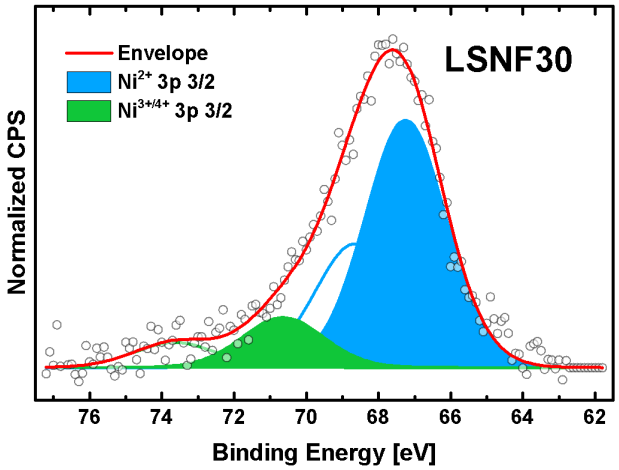

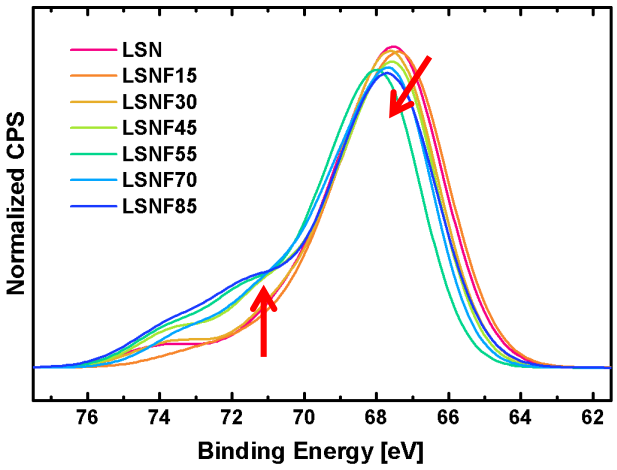

- Ni^{AVG+} calculated from B^{AVG+} (Iodimetric titrations) and deconvoluted Mossbauer spectra
- XPS of Ni 3*p* was collected rather than Ni 2*p* to avoid convolution with La 3*d* emission
- $Ni^{3+/4+}$ peak grows with Fe substitution
- Results are consistent with E_p shift for $Ni^{2+/3+}$

Iodometric titrations performed in triplicate under Ar.

Standardized $Na_2S_2O_3$ was titrated against I_3^-. Samples were dissolved in 6 M HCl.

Forslund, Hardin, et al. *under review* **2017**

DFT+U modeling

DFT+*U* to model PDOS of Ni-O-Fe bridges

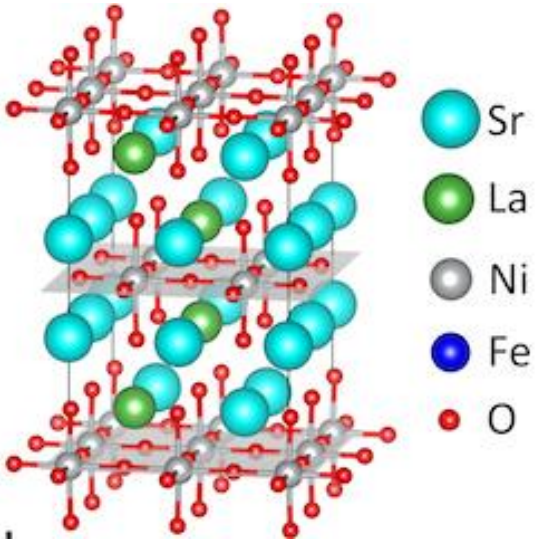

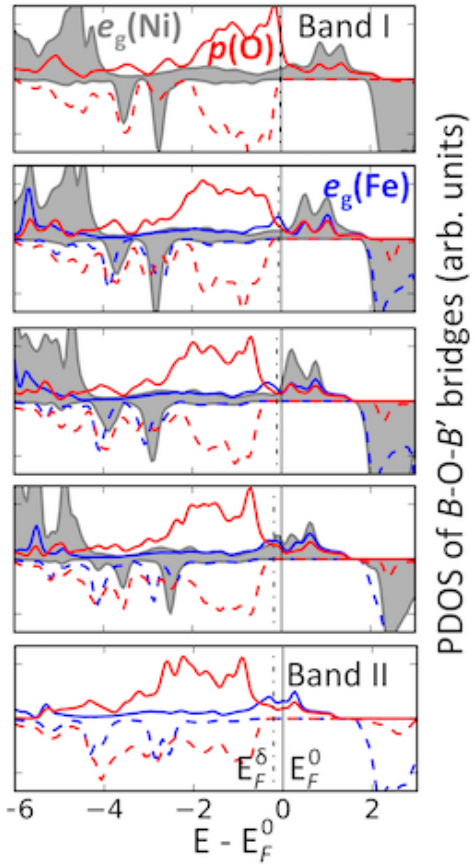

Significant overlap of the Ni e_g^*, Fe e_g^*, and O 2p bands at E_F for all compositions

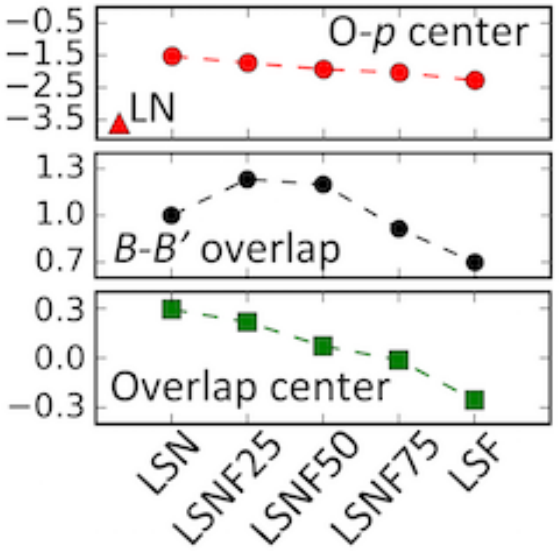

Larger bandwidth → higher density of occupied/unoccupied states around E_F → more surface redox reactions via only slight Fermi level shift → less energetic cost

e_g(Ni) and e_g(Fe) overlap with *p*(O) across the Fermi level: cross-gap hybridization

Forslund, Hardin, et al. *under review* **2017**

Band structure and cross-gap hybridization

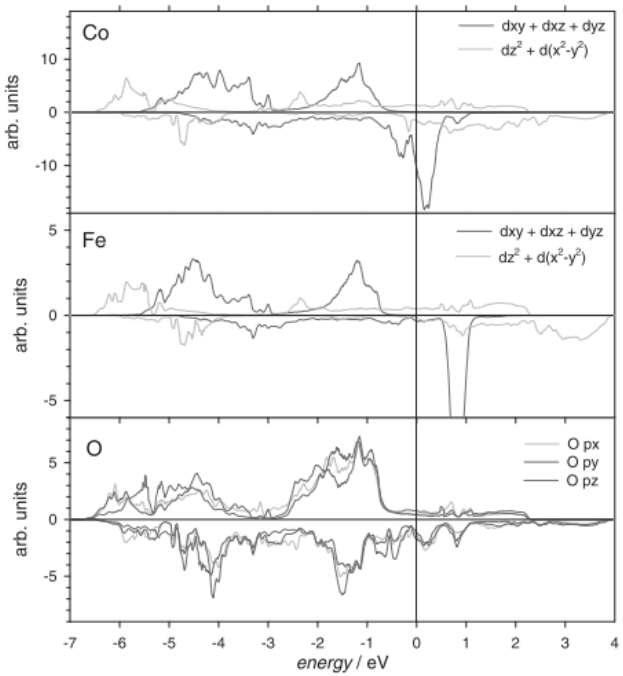

Merkle, *J. Electro. Chem. Soc.* (**2012**) noted similar Co and Fe 3*d* hybridization with O 2*p* across E_F for **$Ba_{0.5}Sr_{0.5}Co_{0.75}Fe_{0.25}O_3$ (BSCF)**

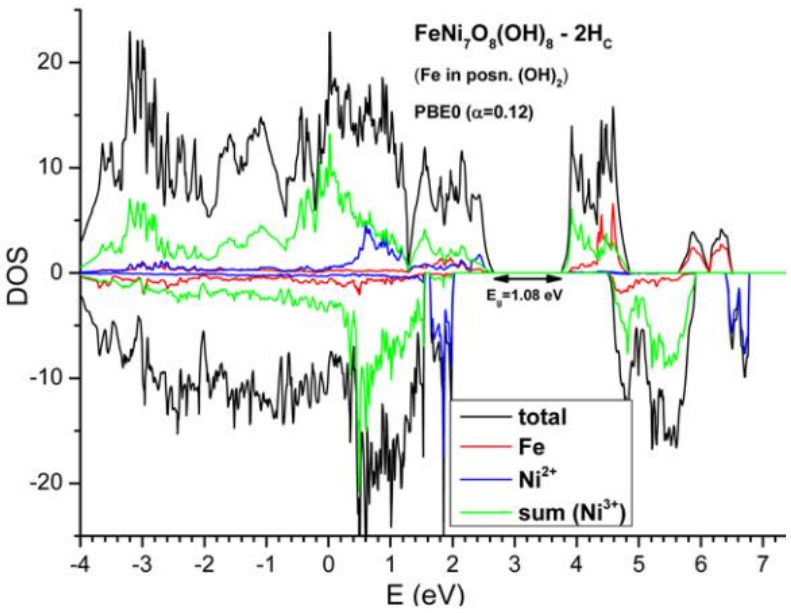

Conesa, *J. Phys. Chem. C* (**2016**) calculated the DOS of a **Ni-Fe oxhydroxide polymorph, FeNi7O8(OH)8** in the $2H_C$ structure with Fe in $O_4(OH)_2$ coordination and their result is strikingly similar to that of LSNF. Ni and Fe 3*d* bands are strongly hybridized just above E_F. They concluded that Fe^{4+} is stabilized by induced charge transfer between Ni sites

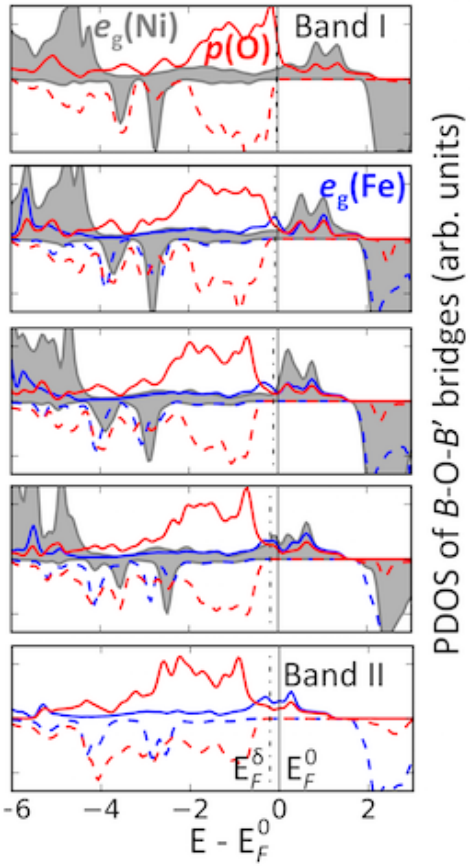

BSCF and Ni-Fe oxyhydroxides exhibit cross-gap hybridization from published band diagrams

Forslund, Hardin, et al. *under review* **2017**

Reducing anodic overpotential

Want to decrease the overpotential for the OER

- Reduce power lost between charging/recharging in metal-air batteries
- **Reduce energy need to make H_2** in electrolyzers

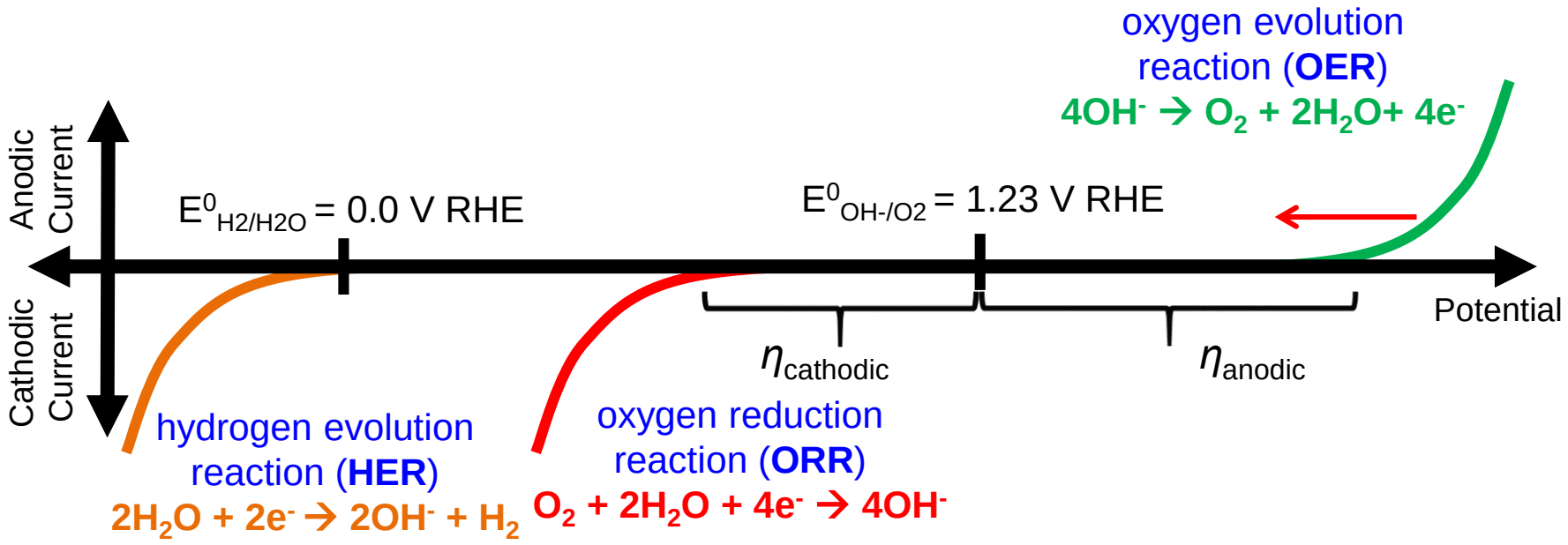

Urea oxidation

Urea is an abundant waste

- Human waste
- Industrial waste
  - Haber-Bosch process consumes 1-2% of world's electricity
    - Fertilizer production waste stream

H_2 generation at a theoretical cell voltage of 0.37 V vs. 1.23 V for water splitting

- Urea oxidation at the anode
- Hydrogen evolution at the cathode

Use a very common waste to generate H_2 using less energy

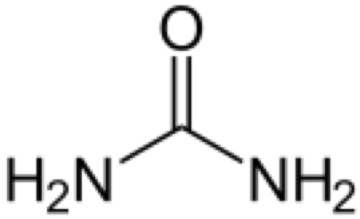

Urea

- Non-toxic
- Non-flammable
- Crystalline solid but readily dissolves in many solvents

Way of remediating potentially hazardous product in waste water

- Urea can break down to form ammonia and nitrates in ground water
- Fertilizer runoff containing urea pollutes lakes and rivers

Urea oxidation

Anode: $CO(NH_2)_{2(aq)} + 6OH^- \rightarrow N_{2(g)} + 5H_2O + CO_{2(g)} + 6e^-$

Cathode: $6H_2O + 6e^- \rightarrow 3H_{2(g)} + 6OH^-$

Overall: $CO(NH_2)_{2(aq)} + H_2O \rightarrow N_{2(g)} + 3H_{2(g)} + CO_{2(g)}$

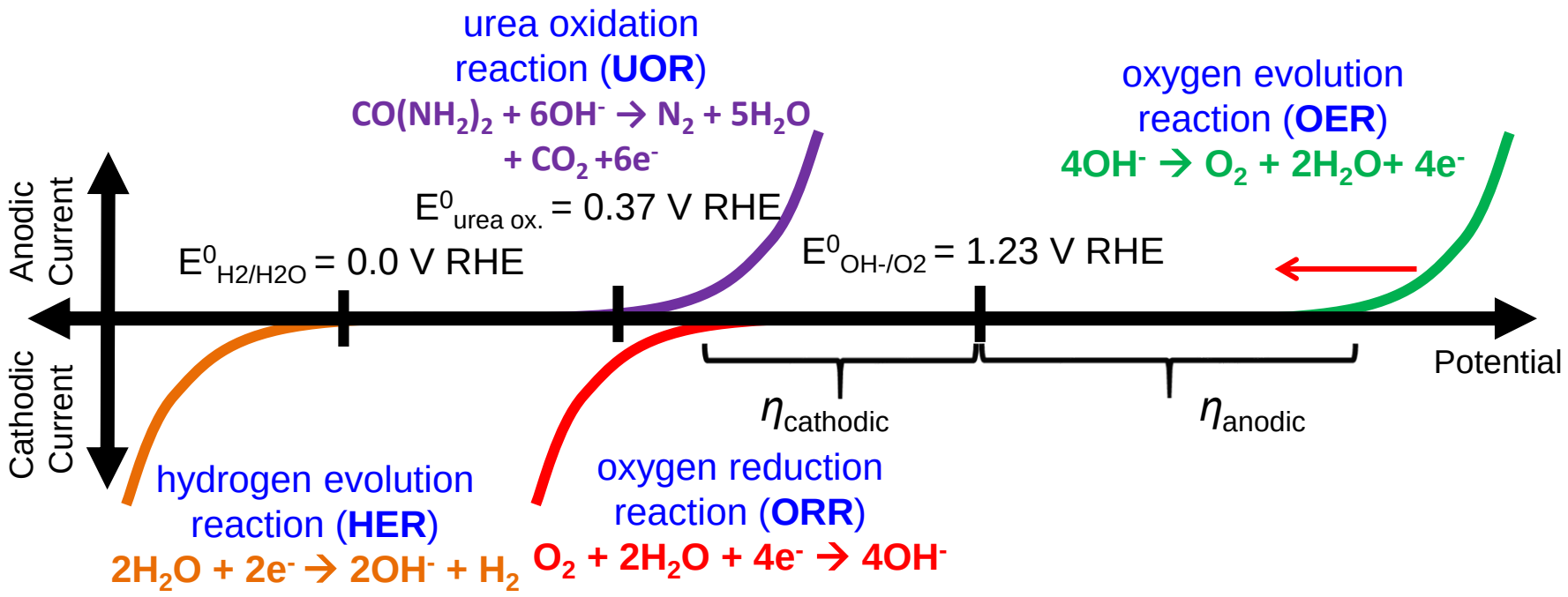

Urea oxidation

Anode: $CO(NH_2)_{2(aq)} + 6OH^- \rightarrow N_{2(g)} + 5H_2O + CO_{2(g)} + 6e^-$

Cathode: $6H_2O + 6e^- \rightarrow 3H_{2(g)} + 6OH^-$

Overall: $CO(NH_2)_{2(aq)} + H_2O \rightarrow N_{2(g)} + 3H_{2(g)} + CO_{2(g)}$

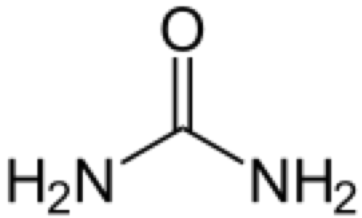

Urea

Ni in various morphologies used by many, EC' mechanism proposed

$Ni(OH)_{2(s)} + OH^- \rightarrow NiOOH_{(s)} + H_2O + e^-$

$CO(NH_2)_{2(aq)} + NiOOH_{(s)} \rightarrow Ni(OH)_{2(s)} + Products$

Use a material where nickel is Ni^{3+} already

Urea oxidation on $LaNiO_3$

$LaNiO_3$

If **A** = La^{3+}

And **C** = O^{2-}

Then **B** = Ni^{3+}

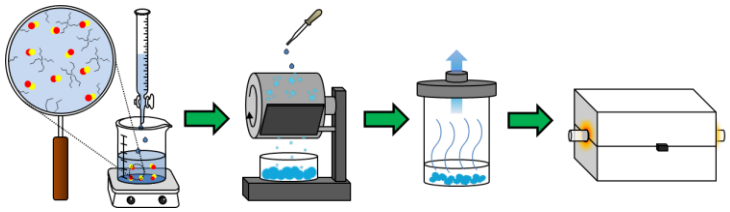

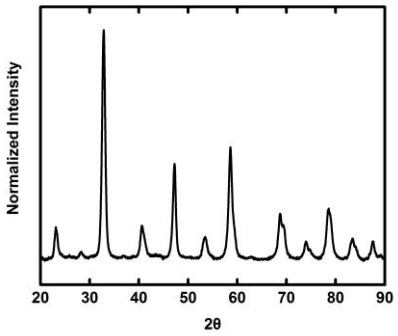

BET surface area 5.5 m^2 g^{-1}

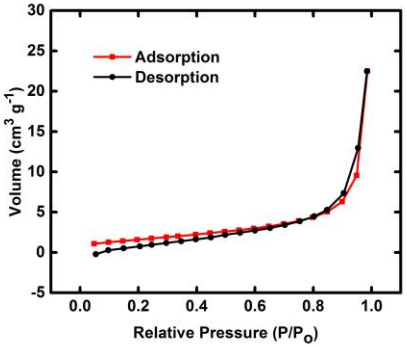

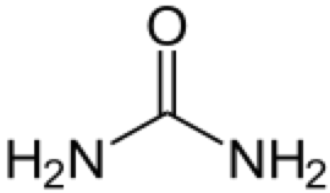

Urea

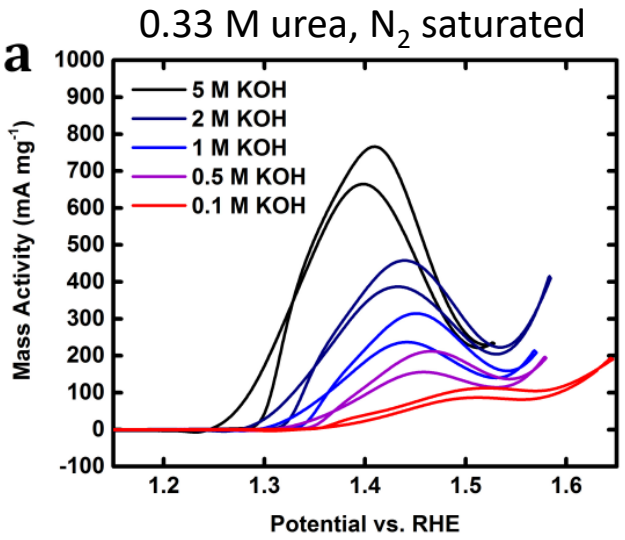

2 Ways to improve catalyst

- Change elemental composition of the perovskite
  - Changing electronic structure may improve catalyst–urea orbital interactions
  - Ni^{2+} → Ni^{3+} → **Ni^{4+}?**
- Increase surface area of the catalyst

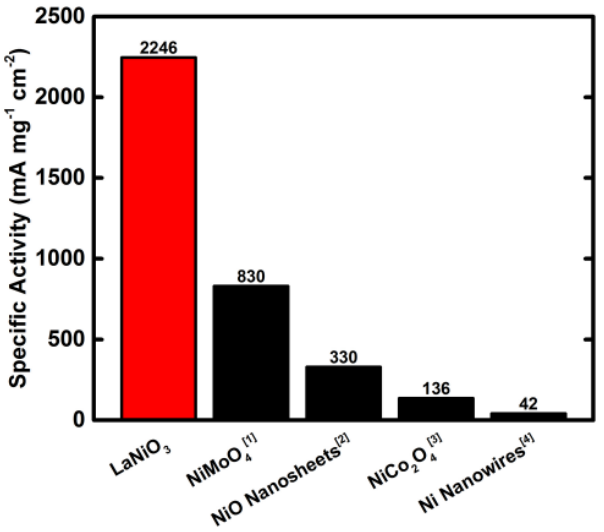

Forslund et al.; *ACS Catal.* **2016**

Urea oxidation on LSN RP

Use the n = 1 Ruddlesden-Popper structure to vary Sr content of $La_{1-x}Sr_xNiO_4$

- Only able to do this in RP structure
- Still not able to do full Sr substitution
- Made 50%, 62%, 75% Sr samples
  - Vary Ni oxidation state from 3 → 3.5 (3.54)

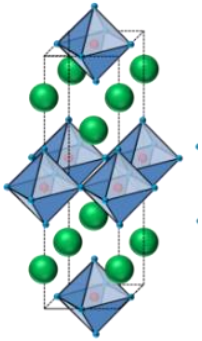

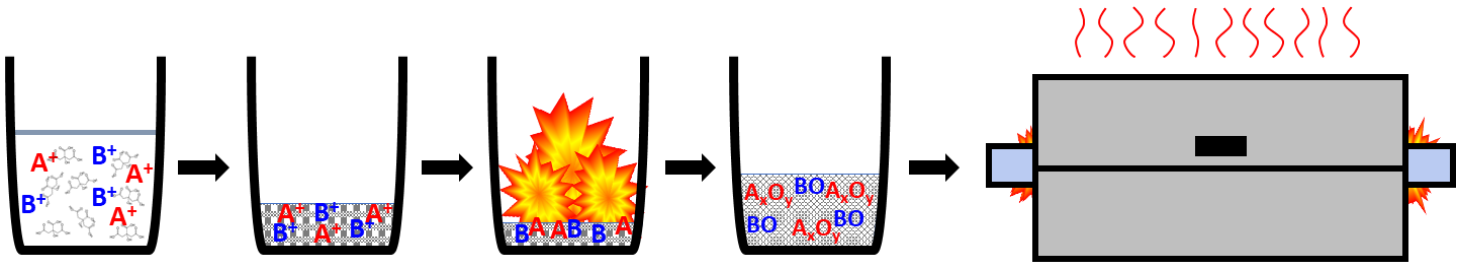

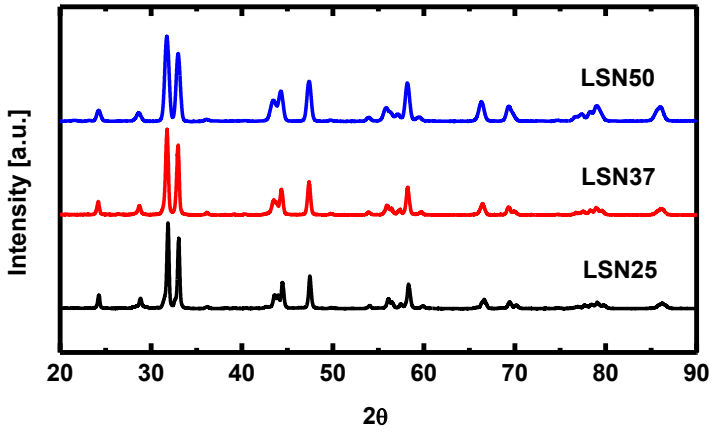

Material	% Sr	Ni Oxidation State
LSN50	50	3
LSN37	62.5	3.25
LSN25	75	3.5

Urea oxidation on LSN RP

Tested in 0.33 M urea, 1 M KOH at 10 mV s^{-1} on stationary RDE electrodes

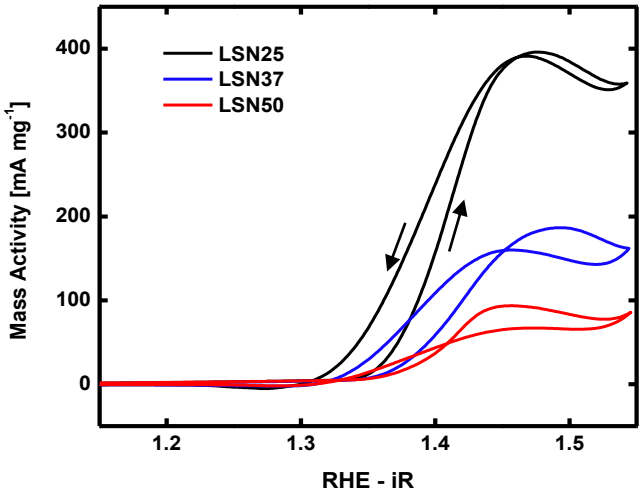

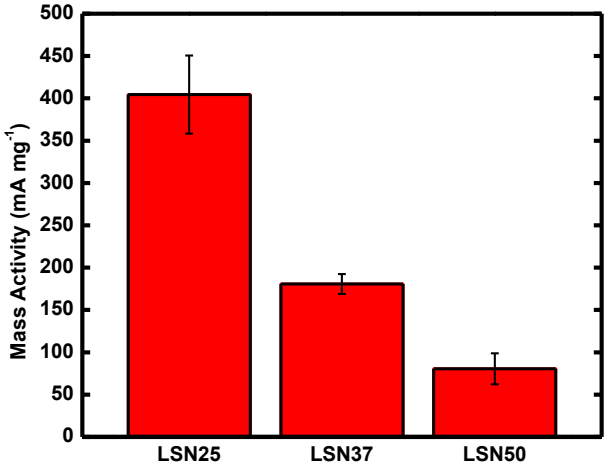

Material	% Sr	Ni Oxidation State
LSN50	50	3
LSN37	62.5	3.25
LSN25	75	3.5

- Increasing Ni oxidation state above Ni^{3+} leads to higher activities
- No shift in onset potential → **no shift in $Ni^{2+/3+}$ redox**

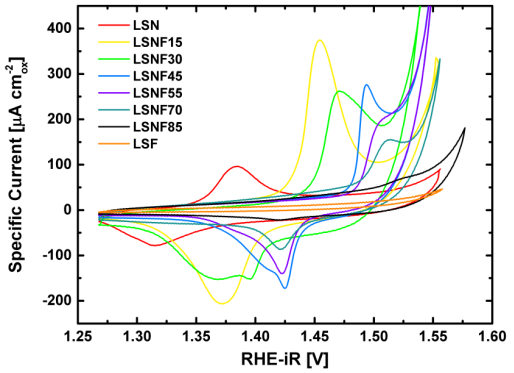

Summary

- Previous work demonstrated importance of M–O bond covalency and the LOM mechanism for the OER
- Chemical substitution in $La_{0.5}Sr_{1.5}Ni_{1-x}Fe_xO_{4+\delta}$ demonstrates the Ruddlesden-Popper phase as highly active for the OER
- Triple-band overlap of Ni and Fe 3*d* states with the O 2*p* (cross-gap hybridization) proposed as new catalytic descriptor for the OER
- Insights into high catalytic activity of Ni-Fe oxyhydroxides and $Ba_{0.5}Sr_{0.5}Co_{0.75}Fe_{0.25}O_3$ (BSCF) are proposed based on cross-gap hybridization
- Urea and other small molecule oxidations provide a path to further lower the potential for the anodic reaction in H_2 generation

Thanks!

Profs. Keith Stevenson and Keith Johnston

Dr. Artem Abakumov

Dr. Alexie Kolpak

Dr. Will Hardin

Dr. Xi (Jerry)

Caleb Alexan

Questions?

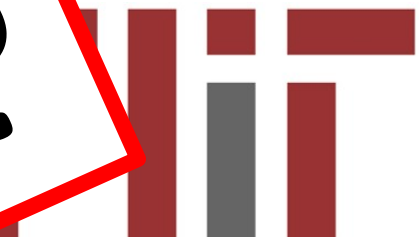

The Welch Foundation

Skoltech